*Quantum Electronics* **49** (11) 989–1007 (2019) 

***REVIEW***

https://doi.org/10.1070/QEL16978

# Coherent beam combining in optically coupled laser arrays

D.V. Vysotsky, A.P. Napartovich

***Abstract.*** **Phase locking of laser arrays is a promising approach for obtaining high-brightness light. A variety of experimental methods have been employed to ensure phase locking. Concurrently, complex theoretical models were developed and nontrivial physical effects were found. Here we review experimental data on passive phase locking and discuss current views on the potentialities of this method.**

***Keywords:*** *phase locking, laser array.*

## 1. Introduction

The modular approach to designing high-power laser systems is very attractive from the technological viewpoint. It allows the total laser output power to be scaled up by combining output beams on a target. In the case of fibre lasers, the beams of individual lasers can be combined in a large-core output fibre. In both cases, the divergence of the combined beam is determined by that of the beams emerging from the individual, small-aperture modules. Since the numerical aperture of the combined output beam typically rises in proportion to the number of modules in the system ($N$), the optical quality of the combined beam is significantly lower than the quality of the beam of a single-mode laser having a total output power equal to the overall power of the laser array and, accordingly, a numerical aperture $N$ times that of one module. The situation can be improved if the fields of all laser modules are coherent with each other. However, in the general case there is an additional requirement that the fields of all beams have the same phase at the output aperture or, at least, that the phase structure of the combined beam remain unchanged over time. In the latter case, the wavefront of the combined field can be flattened by phase correctors. The coherent combining of the output beams of modules allows one, in principle, to raise the axial brightness of the combined beam by $N$ times relative to far-field incoherent beam combining.

An alternative is incoherent laser beam combining techniques (see e.g. Refs [1, 2]). In particular, in the case of spectral combining [3, 4] laser beams of different frequencies are incident on a beam-combining grating at specially adjusted angles such that, after the grating, all the beams propagate in the same direction. Also possible is a multistep system that ensures both spectral beam combining and phase locking [5, 6]. At present, advances in coherent beam combining techniques are ensured by adaptive optics techniques [7, 8] and optical coupling between modules, which leads to spontaneous coherence of the combined field [9, 10].

The oldest approach for obtaining high optical power in conjunction with high output beam quality, employed by Meyman as early as 1960, is optical pumping of a laser by light with poor optical quality. At present, high-power semiconductor lasers with a low output beam quality are widely used as pump sources. This approach has an important advantage over lamp pumping because the laser linewidth is here far smaller, which allows for selective pumping of both gases [11] and solids [12, 13]. The energy efficiency of a laser pumped by another laser can be rather high if one can select similar pump and lasing frequencies. In the case of fibre lasers, use is made of not only optical pumping but also nonlinear processes – stimulated Raman scattering (SRS) [14] and stimulated Brillouin scattering (SBS) [15] – to improve the optical quality of the beam. Since the fundamental mode of fibre has a higher gain than do the higher order transverse modes, the output beam at a Stokes frequency can have high optical quality.

Generally speaking, it is necessary to switch to a modular design of laser systems for any type of laser starting at a certain output power level. The first to encounter this issue were designers of semiconductor lasers at an output power of an individual laser element under 1 W [16]. A natural approach to laser output power scaling is to increase the volume of the active region. Because of the small size of the heterostructure in the direction of the current and the limitation on the diode laser length due to the large gain coefficient, it is necessary to increase the lateral size of the active layer. Direct attempts to increase the lateral size encountered an obstacle in the form of filamentation. Producing a laser array with distributed optical coupling, the segmentation of the active layer in the lateral direction encountered difficulties that have not yet been overcome [17].

At present, the purpose of studies of high-power semiconductor lasers intended to pump solid-state, gas and fibre lasers [11–13] is to maximise their efficiency. In particular, as

**D.V. Vysotsky** Troitsk Institute for Innovation and Fusion Research (State Research Center of Russian Federation), ul. Pushkovykh 12, Troitsk, 108840 Moscow, Russia; Moscow Institute of Physics and Technology (State University), Institutskii per. 9, 141701 Dolgoprudnyi, Moscow region, Russia; e-mail: dima@triniti.ru;
**A.P. Napartovich** Troitsk Institute for Innovation and Fusion Research (State Research Center of Russian Federation), ul. Pushkovykh 12, Troitsk, 108840 Moscow, Russia; e-mail: apn@triniti.ru

Received 22 February 2019; revision received 17 June 2019
*Kvantovaya Elektronika* **49** (11) 989–1007 (2019)
Translated by O.M. Tsarev

part of the DARPA Super High Efficiency Diode Sources (SHEDS) programme (USA) a 500-W diode laser bar with a 70% efficiency was demonstrated [18]. The possibility of directly utilising high-power semiconductor lasers in materials processing and other applications stimulates the development of semiconductor laser systems consisting of separate modules and offering high optical quality of their output beam [19]. In 2005, the goal of the DARPA Architecture for Diode High Energy Laser Systems (ADHELS) programme was formulated: to develop a coherent beam combining technique for semiconductor lasers with a combining efficiency of 80%, output power of ~10 kW and near diffraction-limited beam divergence ($M^2 = 1.2$) [18].

In some gas lasers, huge power levels were reached in a quasi-cw mode [20, 21], but the output beam quality was markedly poorer than the diffraction limit, thus limiting their potential applications. Examples of the phase locking of gas laser arrays were examined in a review by Glova [10]. In recent years, significant advances have been made in beam brightness scaling of diode-pumped solid-state lasers owing to the transition to a thin-disk gain element geometry [22, 23]. Mende et al. [24] discussed the feasibility of a transition to a modular design based on such elements, with subsequent beam combining.

In fibre lasers, a transition to multistep systems having a large core area amplifier as the final stage allowed a single-mode power level of ~10 kW to be reached. Note that the output stage of amplification at a wavelength $\lambda = 1070$ nm can be pumped by a fibre laser at $\lambda = 1018$ nm [25] (tandem pumping scheme). A detailed analysis of the factors limiting the single-mode lasing power level was presented by Dawson et al. [26] for an Yb-doped fused silica fibre amplifier. In particular, at a fibre length of 40 m and core diameter of 90 μm, the maximum laser output power was estimated at 36.6 kW for a multimode amplifier and 1.86 kW for a single-frequency amplifier at a pump brightness of 0.021 W $\mu^{-2}$ $sr^{-1}$ [26]. As the fibre length increases, SRS and/or SBS becomes a limiting factor, whereas increasing the diameter of the active core makes thermal lensing a limiting factor. An increase in pump brightness by five times would allow the same output power to be reached at a fibre length of 10 m and core diameter of 60 μm. The output power would then be limited by the optical damage threshold of the glass. In the case of short pulse amplification, the peak power is much higher, so self-focusing processes [27] and re-emission to other modes of the fibre come to the fore.

Fibre laser beam combining has been the subject of very extensive studies (see a review by Augst et al. [28]). A noteworthy feature of fibre lasers is that their active cores differ in characteristics at a long fibre length, which leads to an uncontrolled scatter in phase shift at a given frequency, up to hundreds of radians. In such a situation, the problem of passive phase locking of the fields of all lasers should be examined in terms of probability theory [29, 30].

The simplest approach for combining single-mode modules into an array is to use a master oscillator whose output beam is split into several beams, which are then launched into a set of amplifier modules (Fig. 1a). Since the amplifier modules differ in optical properties, the channels differ in phase shift, which leads to a reduction in coherent beam combining efficiency. Such a scheme can find application only at a small difference in phase shift between the amplifiers involved (see e.g. Glova et al. [31]). An increased scatter in field phases in the amplifiers can be compensated for [32] via reflection from a mirror with wavefront conjugation (WFC) of the combined beam and subsequent beam propagation through the amplifier system in the opposite direction. It is also worth noting a report by Bogachev et al. [33], who effectively utilised phase-conjugate mirrors supplemented by systems of Fresnel lenses for phase compensation in a system of four parallel amplifiers.

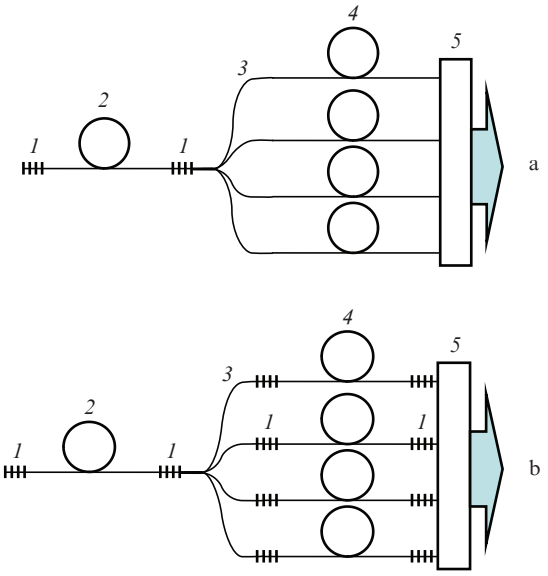


**Figure 1.** Schematics of (a) a fibre laser with a system of amplifiers and (b) a system of lasers locked to a master oscillator: (*1*) Bragg reflector; (*2*) master oscillator; (*3*) coupler; (*4*) amplifiers; (*5*) output coupler.

Master oscillator signal injection into a system of lasers (Fig. 1b) involves the problem of locking stability in the lasers. The eigenfrequencies of the master oscillator and slave lasers should be matched with high accuracy.

The purpose of this work is to discuss the current state of the art in passive coherent laser beam combining, taking into account the specifics of various types of lasers. Section 2 addresses general issues pertaining to optical coupling in a laser array and a number of approaches for ensuring it. In Sections 3 and 4, we examine locking methods for multichannel lasers with distributed diffractive coupling (DDC) and Talbot filters, respectively. Section 5 describes theoretical models that are employed in calculations of laser arrays. Finally, in Section 6 we discuss possible operation modes of an optically coupled laser array.

## 2. Optical coupling schemes

Interaction between lasers via diffractive field exchange was first considered by Basov et al. [34], using two lasers with closely spaced Fabry–Perot cavities as an example. Subsequently, Perel' and Rogova [35, 36] derived dynamic equations for fields in a system of two resonators coupled via a semi-transparent mirror, with an active medium present in only one resonator. The stability of one common laser mode was analysed by Spencer and Lamb [37]. As shown by Likhanskii and Napartovich [9] for a laser array, the generation of a common supermode is most stable to scatter in

eigenfrequencies if the lasers are coupled to each other with identical coupling coefficients (another name is global coupling [38]). Bondarenko et al. [39] were the first to experimentally demonstrate the development of the self-oscillation regime as the optical coupling strength between two $CO_2$ lasers decreases because of the detuning of the eigenfrequencies of their cavities. A detailed survey of early research into the operation of two optically coupled lasers can be found in Ref. [9] and a paper by Roy [40], who discussed the phase locking of lasers in chaotic mode as well.

The kind of optical coupling between laser elements depends on the type of laser. In the case of multielement semiconductor and fibre lasers, designs were demonstrated with diffractive field exchange between neighbouring elements during light propagation [16, 41, 42]. If diffractive exchange is low effective (for example, at a large optical mode area), field exchange between different lasers can be ensured by a special external device. In particular, Veldkamp et al. [43] proposed using a transparent diffraction grating with identical emission intensities in different orders of diffraction. The grating made by them had a 75% efficiency for splitting a beam into seven diffraction orders and was used to couple two or three He–Ne lasers. In an experiment with an analogous grating and an additional filtering aperture in the far field, Leger et al. [44] demonstrated the locking of six out of ten elements of a diode bar with a 68% efficiency. Morel et al. [45] reported the phase locking of three fibre lasers with a 70% efficiency.

Recently [46], five semiconductor lasers were locked using a diffraction grating that split an input beam with a 98% efficiency. An analogous grating combined the beams emerging on the other facet of the bar. At a current of 4 A, the power in the zeroth order of diffraction was 6 W and remained constant in time. At a current of 5 A, it was 7.5 W out of the 12 W of total power, but lasing became unstable. Subsequently, Schimmel et al. [47] proposed separating the problems of beam combining and phase locking using a semiconductor laser with a distributed feedback grating as a master oscillator. As a result, stable phase locking persisted up to a current of 6 A and was ensured by an output power of 11.5 W in the zeroth order of diffraction at a combining efficiency of 78%. As the next step in the development of the concept, a system for active phase shift tuning in amplifying channels was added to a multichannel amplifier, in which a diffraction grating was only used for combining its output beams into a single beam. Owing to the high quality of diffractive optical elements in such systems, Redmond et al. [48] and Thielen et al. [49] demonstrated beam combining into a beam with a quality factor $M^2 = 1.1$ from five fibre amplifiers with an efficiency of 79% and power of 1.93 kW and from a $3 \times 5$ two-dimensional (2D) amplifier array with an efficiency of 68% and power of 600 W, respectively.

The out-of-phase mode of an array has two main beams in the far field, which diverge at an angle $\lambda/(2\Lambda)$ with respect to the optic axis, where $\Lambda$ is the period of the structure. Placing an angle-selective mirror, which returns only the field of one of the beams, one can ensure lasing only on this mode [50].

To date, a number of approaches have been employed to ensure optical coupling between lasers through field rescattering by spatial amplitude filters, whose part can be played as well by the periodic structure in the arrangement of amplifiers in a laser array [9].

### 2.1. Optical coupling through a filter in the focal plane

A priority issue in laser engineering is the ability to minimise the far-field intensity distribution width, so a natural way of selecting supermodes is by filtering the field distribution in the focal plane of a lens or mirror in the output section of the system. To minimise the beam divergence of a large-aperture solid-state laser in their experiments, Gerasimov et al. [51, 52] used a limiting circular diaphragm in the focal plane of one of its mirrors, which selected out the laser mode with the smallest far-field divergence, suppressing all other supermodes. He et al. [53] demonstrated phase locking of radiation from two fibre lasers with a 88% efficiency with the use of a focal filter. Wan et al. [54] presented a detailed numerical analysis of how parameters of a focal filter influence supermode separation selectivity in systems of two and three lasers. In such geometry, however, the edge of the diaphragm is exposed to high-power radiation and one loses the field in side diffraction orders in the focal plane. These drawbacks were partially overcome in experiments reported by Aleksandrov et al. [55], where the radiation from a $CO_2$ laser array was phase locked by passing it through a diaphragm with a system of holes corresponding to maxima in the far-field intensity distribution of the in-phase mode. An analogous spatial filter was used by Rediker et al. [56] to phase-lock the radiation from an array of five semiconductor lasers.

Fridman et al. [57] studied a $5 \times 5$ array of fibre amplifiers differing in length and coupled through a system of mirrors in the focal plane. At the output in the far field, they observed radiation with a rapidly varying brightness. In addition, at the instants corresponding to the average axial brightness the far-field intensity distribution corresponded to the output of one laser, whereas at the instants corresponding to maximum brightness they observed the structure of a combination of supermodes of the array. In the case of a 2D square array, the time-averaged efficiency decreased from 90% for 3 lasers to 29% for 25 lasers, but 90% locking efficiency was reached for some time even at a larger number of lasers ($N$): 0.1% of the time at $N = 12$, 0.012% at $N = 16$, 0.004% at $N = 20$ and 0.001% at $N = 25$. In addition, Fridman et al. [30] showed that, under the experimental conditions of their study, the average size of a cluster of locked lasers had a Gaussian probability distribution with a mean size of $\sim 7$.

For a fibre laser array, single-mode fibre can be used as a spatial filter, with a small part of the output beam of a system of fibre amplifiers focused onto its input end [58]. The field produced in the single-mode fibre is delivered to the input of the amplifier system to form a common ring cavity (Fig. 2). Separating the in-phase mode in such a laser configuration, Shalaby et al. [59] achieved the phase locking of fields in an active 19-core fibre. To demonstrate the feasibility of the phase locking of two multicore lasers in a ring cavity configuration, Shalaby et al. [60] imitated lasers by two parallel passive seven-core structures and a common amplifier based on single-mode fibre, which served as a spatial filter as well. In those experiments, the in-phase mode separation efficiency was above 95%, but the fraction of the power coupled into the single-mode fibre was far below 1%.

To improve the efficiency of common supermode separation in ring geometry, Yang et al. [61] proposed placing a diffraction grating between a focusing lens and single-mode fibre, so that the beams from three separate amplifiers propagated in diffraction order directions of the grating. Even

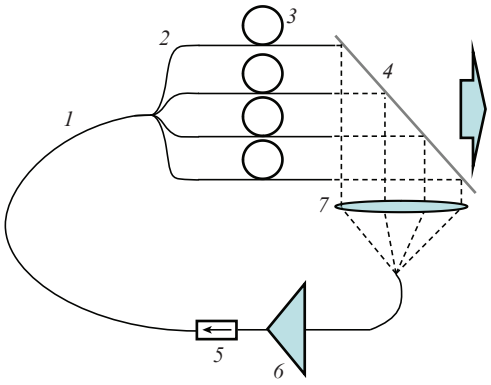


**Figure 2.** Schematic of a cavity with single-mode fibre filtering: (*1*) single-mode fibre; (*2*) 1–*N* coupler; (*3*) fibre amplifiers; (*4*) semitransparent mirror; (*5*) optical isolator; (*6*) preamplifier; (*7*) lens.

though the efficiency of beam combining on the grating was relatively low, 61%, they demonstrated phase locking with 20 W of output power. In this process, 1.5 mW of power was coupled into the fibre.

At high output powers, most of the light leaves the ring cavity. Since the optical fields in the individual amplifiers are phased, output beams can be combined on a diffraction grating. Using such a configuration with three fibre amplifiers, Liu et al. [62] obtained 206 W of output power at a beam quality factor $M^2 = 1.38$.

### 2.2. Fourier coupling

A natural development of the far-field filtering method is the use of the output end faces of a laser array as a selecting aperture in the Fourier plane (Fig. 3). The image at the focus of a lens coincides with the structure of the emitting laser end faces under the condition that $\Lambda^2 = \lambda F$, where $F$ is the focal length of the lens. Such a compound cavity with Fourier coupling was first used by Corcoran and Rediker [63] to phase-lock five fibre-coupled semiconductor lasers. Later, an analogous configuration was used to phase-lock seven fibre lasers [64]. The theory of phase locking of a Fourier-coupled laser array is discussed in Section 5.

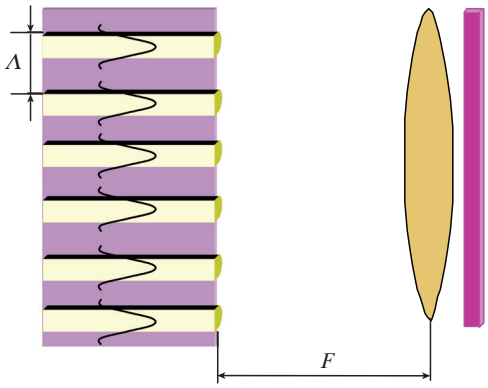


**Figure 3.** Schematic of a cavity with Fourier coupling.

### 2.3. Optical coupling through nonlinear cells

Field coupling of two lasers in four-wave scattering processes in nonlinear cells was first considered theoretically by Likhanskii et al. [65] and demonstrated experimentally in gas lasers with different nonlinear cells by Baranov et al. [66] and Bondarenko et al. [67]. Beams counterpropagating in an active medium produce gain gratings, which allows gain elements to be used as coupling cells based on the four-wave scattering effect [68, 69]. Basiev et al. [70, 71] demonstrated coupling of two and three Nd:YAG lasers in such geometry. In the latter case, they obtained pulses with an energy of 0.94 J at a wavelength of 1.34 μm and a repetition rate of 10 Hz.

### 2.4. Interference coupling

If two fibre lasers are coupled by a $2 \times 2$ coupler and reflection from the fibre end face is eliminated in one of the coupler ports, such a compound cavity, equivalent to a Michelson interferometer, will ensure frequency tuning of the lasers to a common lasing frequency at which the loss due to emission through the open port will be zero [72]. Theoretically, sequential pairwise coupling with couplers allows any number of lasers to be coupled to each other. In experiments, stable coupling of seven or eight fibre lasers with a relatively low power was demonstrated [73, 74]. The drawbacks to this approach are that the output of the entire array is coupled into single-mode fibre and that lasing is unstable in time [75]. Bruesselbach et al. [76] experimentally studied a system of ten lasers, each with an output power of ~100 W in the case of independent lasing. According to their results, eight lasers can be successfully phase-locked at a low output power, whereas increasing the array to nine or ten lasers leads to a reduction in phase locking efficiency ($\eta$), determined as the fraction of the power outcoupled through output fibre. At an increased power, the efficiency drops sharply as the number of coupled lasers increases.

Wang et al. [77] studied coherent combining of two large mode area fibre laser beams in a configuration with interference coupling. At an individual laser power of ~27 W, an output power of 50.1 W was reached ($\eta = 92.8\%$). Reducing the active core size led to a more rapid decrease in efficiency with increasing power. As the difference in optical length between the lasers was increased, $\eta$ became independent of pump power. Kabeya et al. [78] studied in detail the reduction in $\eta$ with increasing pump power in a two-arm ring fibre laser system. It was shown that $\eta$ decreased to 90% and that the emission spectrum at the loss port followed the phase-locked emission spectrum except in narrow regions near peak positions in the latter spectrum. To interpret this effect, it was assumed that, at a high pump power, the width of the mode spectrum was determined by the gain band and the fraction cut from the emission spectrum by the external coupling system gradually decreased.

Multiple-beam interferometer geometry with a system of semi-transparent mirrors was successfully used by Ishaaya et al. [79] to couple 16 solid-state amplifiers. Zhao et al. [80] coupled three Nd:YAG lasers in an interferometer with additional far-field filters. As a result, a single beam with $M^2 = 1.35$, containing 76% of the energy (124 W) in the central maximum, was obtained instead of three output beams with $M^2 = 5.5$. For semiconductor lasers, interference coupling

was ensured by rotating the plane of polarisation of half of the beams and then bringing them together using a birefringent plate. Phase-coupling four lasers in this way, Purnawirman and Phua [81] reduced their output power from 10.2 to 7.2 W and their lateral $M^2$ factor by 20 times.

## 3. Distributed diffractive coupling

DDC systems include semiconductor laser bars (integrated arrays) and multicore fibre lasers in which field exchange between elements occurs through diffraction of light.

### 3.1. Semiconductor lasers

Early work on the phase locking of diode laser arrays was reviewed by Goldobin et al. [16] and Botez [41], and that on lasing dynamics, by Winful and Defreez [82]. It became clear as early as the 1980s that diode laser bars, consisting of active waveguides separated by passive regions with a lower refractive index (RI), were unsuitable for the stable phase locking of the in-phase mode [41]. As a result of the optical loss in interelement gaps, weak optical coupling due to the rapid decrease in the field tunnelling from active fibres and variations in RI due to heating of the contact and changes in carrier concentration in quantum wells, the out-of-phase mode prevails or single-mode lasing becomes unstable with increasing pump current.

Advances in single-mode diode bar scaling were made after a transition to antiguided structures with gain regions separated by passive waveguides. Optical coupling in such structures is ensured by travelling waves and, provided there is resonance wave propagation through interelement gaps, is similar in properties to global coupling [41]. In an antiguided 20-element laser bar, stable in-phase mode lasing was obtained with 500 mW of power in continuous mode [83] and 2 W in pulsed mode [84]. In a 40-element laser bar, Yang et al. obtained 10 W of power in pulsed mode [85] and 1.6 W in continuous mode [86] at a beam divergence exceeding the diffraction limit by a factor of 2 and 1.8, respectively.

In vertical-cavity surface-emitting lasers (VCSELs), stable phase locking was obtained in square antiguided arrays consisting of 100 [87] and 400 [88] elements. In recent years, the advent of quantum cascade lasers has revived interest in antiguided laser bars. Kirch et al. [89] demonstrated a five-element bar with 5.5 W of output power at a wavelength $\lambda = 8.35$ μm in pulsed mode. Note that the central peak, with a divergence exceeding the diffraction limit by a factor of 1.65, accounted for 4.5 W of power. At $\lambda = 4.7$ μm, Sigler et al. [90] obtained 3.6 W of peak output power in a five-element laser bar with diffraction-limited beam divergence.

### 3.2. Fibre lasers

One way of increasing the fundamental mode area in fibre lasers is by using multicore structures. In pioneering work by Glas et al. [91], to raise the pump absorption coefficient the centres of 38 circular active cores 6.9 μm in diameter were arranged on a 115-μm-diameter circle near the outer fibre cladding. According to calculation of core coupling constants in this configuration [92], diffractive field exchange between neighbouring cores will occur over a propagation distance of ~1.3 mm. Experimental data demonstrate that, nevertheless, such coupling is insufficient for phase-locking the fields in the cores.

Huo et al. [93, 94] demonstrated the operation of fibre lasers with hexagonal arrays formed by 7 and 19 active cores, respectively, with a diameter of 7 μm and a period of 10.5 μm. They observed spontaneous phase locking of the fields in the cores as the pump power was raised.

A hexagonal structure of active cores was also studied in photonic crystal fibres with an ordered array of air holes, which formed a 2D photonic crystal with defects containing active components. The technology and properties of microstructured fibres were discussed in a review by Russel [95]. In a photonic crystal fibre laser [96] having six ytterbium-doped active cores, single-mode generation of pulses 26 ns in duration and 2.2 mJ in energy was achieved at a mode area of 4200 μm$^2$. Using such fibre, with seven cores, as a final amplifier in a standard pulse stretching–amplification–compression scheme, Fang et al. [97] obtained 110-fs pulses with a peak power of 150 MW and mode area of 5000 μm$^2$. Fang et al. [98] utilised a photonic crystal fibre with 18 active cores as an amplifier in a passively $Q$-switched laser. Its output had a relatively high optical quality ($M^2 = 1.52$). Next, the pulses were compressed by an external system to a duration of 690 fs. These results suggest that multicore fibre is promising for the generation of microjoule pulses shorter than 100 fs at a repetition rate of 50 MHz [99].

Beach et al. [100] proposed a ribbon fibre structure comprising a periodic sequence of active and passive segments (Fig. 4a), embedded in a reduced-index cladding region. According to calculations for a five-element structure with a varied index difference between the active and passive regions, such a structure is most effective at an index modulation under 0.001. The theoretical predictions were confirmed by experimental data [101] for a waveguide amplifier with five Nd-doped active cores, in which an in-phase mode with a uniform intensity distribution was realised.

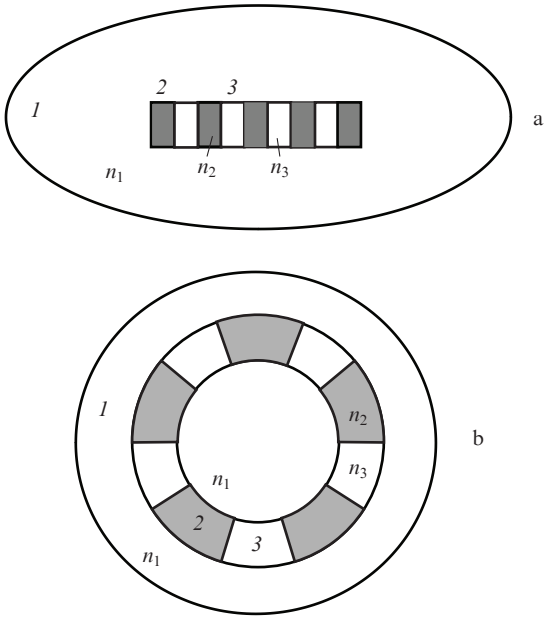


**Figure 4.** Schematic of fibre with (a) a planar and (b) a circular ribbon waveguide [107]: (*1*) cladding; (*2*) active core; (*3*) passive section of the ribbon waveguide; $n_{1-3}$ are the corresponding RIs ($n_3 \geqslant n_2 > n_1$).

The structure analysed by Beach et al. [100] is similar to that of antiguided semiconductor laser bars [41], differing only in that there is no absorption in the passive sections and that the edges of the structure have high reflectivity. Theoretical analysis by Vysotsky et al. [102] generalised the results presented in Ref. [100] and included the case of a large index difference between the active and passive regions. The latter is important for practical applications because the index difference determines the acceptable processing-induced scatter in RI. They derived explicit expressions for the maximum higher mode discrimination level and the largest number of phase-locked cores. For a resonant antiguided ribbon fibre laser structure, higher mode discrimination was independent of the number of elements up to ~1000 elements.

Dawson et al. [103] proposed increasing the ribbon structure thickness by adding thin increased-index layers, which would allow a mode with a flat intensity profile across the ribbon to be produced in each element. Mode profile flattening raises the threshold power for nonlinear processes and allows the single-mode lasing output power to be increased.

Drachenberg et al. [104] demonstrated multimode operation of a ribbon waveguide laser with an output power of 40 W and beam spot area of 600 $\mu m^2$. To achieve single-mode operation, the fibre was used as an amplifier with single-mode light injection [105]. An alternative approach is to place an external filter in the far field. As demonstrated by Anderson et al. [106], the use of a bulk Bragg grating with an angular reflection bandwidth of 4.7 mrad as an external mirror allows the output beam quality to be improved to $M^2 = 1.45$. This is accompanied by a drop in the optical efficiency of the laser from 76% to 53%.

A further development of the ribbon fibre laser concept is the structure represented in Fig. 4b [107]. Here, the active structure has the form of a ribbon waveguide rolled around the fibre axis and having alternating increased- and reduced-index regions. The reduced-index regions contain active dopants (Er, Yb and others). This design allows one to sharply increase the optical mode area, while maintaining a high degree of fundamental mode selection. Calculations [108] show that, in the case of a ring waveguide (RW) having seven active sectors, an inner radius of 18.5 μm and outer radius of 34.5 μm, the in-phase mode can be reliably selected at index differences in the range $0.0015 < \Delta n < 0.0025$. The addition of circular passive layers with an RI exceeding that of the active elements will lead to the same advantageous effects as were predicted by Dawson et al. [103] for a ribbon laser.

The sliced slab $CO_2$ laser design reported by Sha et al. [109], with a laterally modulated RF pumping and weak index modulation, is in effect of the same type as the ribbon fibre laser design. Sha et al. [109] demonstrated the phase locking of ten overlapping laser beams, so that the far-field intensity distribution had one peak, without sidelobes.

## 4. The use of the Talbot effect

In 1836, Talbot [110] discovered the reproduction of periodic structures at a certain distance (referred to as the Talbot distance, $L_T$) from an emitting aperture. The effect was explained in 1881 by Rayleigh [111]. Antyukhov et al. [112] proposed using the self-reproduction of a periodic field distribution for the phase locking of a hexagonal array formed by 56 waveguide $CO_2$ lasers. Phase locking efficiency, determined as the ratio of the output powers obtained with the external plane mirror placed distance $L_T/2$ from and next to the waveguide end facets, was 20%, but the far-field axial brightness increased by ten times. Along with an in-phase supermode, a mode with phase modulation was found experimentally. Later, Golubentsev et al. [113] showed theoretically that, in the case of an infinite hexagonal laser array, three modes were exactly reproduced at the Talbot distance [$L_T = 3\Lambda^2/(2\lambda)$]: in-phase mode and two modes with phase modulation in a triangular unit cell (Fig. 5b). If the arrangement of laser end facets has square geometry, along with a constant-phase field distribution an additional three supermodes are reproduced at a distance $L_T = 2\Lambda^2/\lambda$ (Fig. 5a).

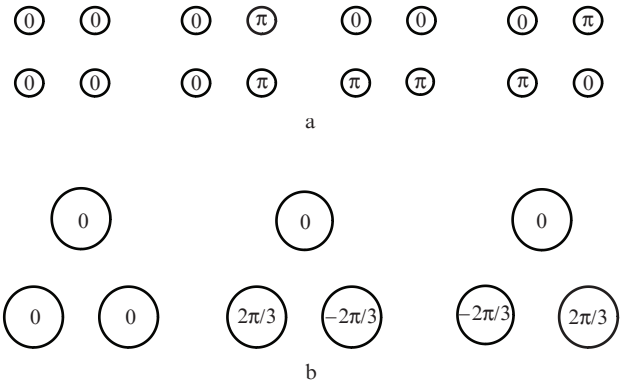


**Figure 5.** Self-reproducing modes in a unit cell of infinite (a) square and (b) hexagonal arrays [113].

In an infinite 1D laser array, the periodic field structure is exactly reproduced over the Talbot distance for both the in-phase and out-of-phase modes. At a distance $L_T/2$, the image of the out-of-phase mode is identical to the parent image, whereas the image of the in-phase mode is displaced by half a period relative to the parent structure, i.e. the external Talbot cavity of length $L_T/4$ selects the out-of-phase mode. Field phases at the output aperture can be compensated for by phase correctors with an optical thickness equal to half the wavelength [114].

The shift of the image of the in-phase mode at a distance $L_T/2$ can be compensated for (Fig. 6a) by an appropriate tilt of a mirror placed at a distance $L_T/4$. In this manner, the in-phase mode was selected in 1D arrays of gas [115] and semiconductor [116] lasers.

The shift of the image of the in-phase mode of an emitter array by half a period at a distance $L_T/2$ was also utilised in a study by Mawst et al. [117], where two antiguided semiconductor laser bars, each having ten cores, spaced distance $L_T/2$ apart along the optic axis, were displaced relative to each other by half a period (Fig. 6b). As a result, they were able to concentrate ~75% of the output power in the central peak in the far field. An analogous scheme was used by Jia et al. [118] to phase-lock an array of 11 quantum cascade lasers. Stable in-phase mode lasing was demonstrated at a current almost twice the threshold one.

For a circular active medium, Napartovich et al. [119] proposed using the difference between the images of the in-phase and out-of-phase modes of arrays by rotating periodically segmented plane mirrors forming a common cavity

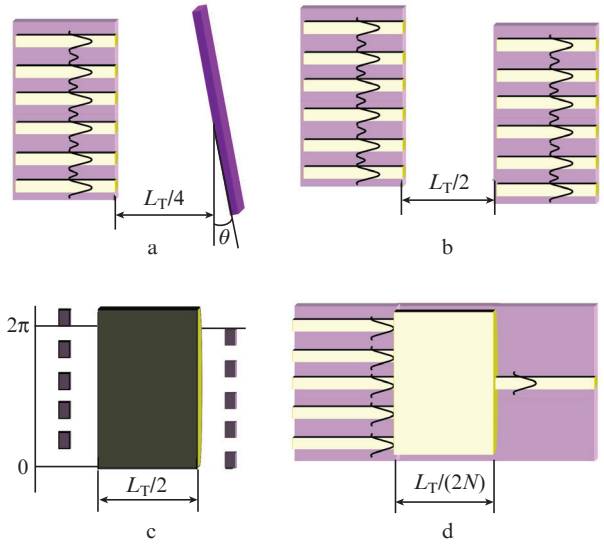


**Figure 6.** In-phase mode selection schemes utilising the Talbot effect: (a) external filter with a mirror inclined at an angle $\theta$; (b) two integrated arrays displaced laterally by half a period; (c) active RW of length $L_T/2$ with two sector mirrors tilted by half an angular period; (d) 1–$N$ scheme.

through half a period (Fig. 6c). Numerical simulation of a $CO_2$ laser having the described compound cavity predicts stable in-phase supermode lasing at a pump power 70% above threshold. This cavity design has not yet been verified experimentally.

In a plane corresponding to a fraction of the distance $L_T$, supermodes differ in structure, and the loss degeneracy of the supermodes can be lifted using a spatial filter [120]. This approach was used to phase-lock a linear array of seven semiconductor lasers [121]. In a study by Golubentsev et al. [122], a Talbot filter in the form of a metallic grating placed in one of the field reproduction planes outside the focal plane of an external forming system phase-locked the radiation from a square array of 36 waveguide $CO_2$ lasers with a phase locking efficiency near 60%. Displacing the filter in a transverse plane allowed various supermodes of the array to be selected. In a hexagonal array of 85 waveguide $CO_2$ lasers, in-phase supermode lasing was demonstrated experimentally by filtering the overall field in a plane spaced distance $L_T/3$ apart from the array [123].

Using masks, Tradonsky et al. [124] imitated a square array of 450 lasers, a triangular array of 1050 lasers or a hexagonal array of 700 lasers in a cylindrical Nd:YAG crystal 10 mm in diameter. To raise degeneracy, an additional filter comprising two lenses and an aperture in the focal plane was placed in the far field behind an external Talbot filter. One mode of the array was observed in all cases.

A distinctive feature of the in-phase mode is that its wavefront is perpendicular to the optic axis, whereas the radiation of the out-of-phase mode comprises two components, with a rather large angle between them in the case of semiconductor laser bars. The in-phase mode can be selected by placing not a conventional mirror, but a bulk Bragg grating with a high angular selectivity of reflection at a distance $L_T/4$ [125]. Using such a scheme, Liu and Braiman [126] recently demonstrated the phase locking of a linear array of ten semiconductor lasers with 4.8 W of output power.

An obvious problem related to the use of the Talbot effect for phase-locking a real laser array is that periodicity conditions are violated at the edges of the array. To compensate for boundary effects, it was proposed to use phase compensators [127] or a stable resonator instead of a plane-parallel one [128], but to the best of our knowledge there was no experimental verification. As shown theoretically [129] and experimentally [130], the Talbot effect takes place as well in a planar waveguide with perfectly reflective lateral walls. In integrated optics, this effect is thought of as a particular case of multimode interference (see the reviews in Refs [131, 132]). Recent results demonstrate the phase locking of linear arrays of three [133] and six [134] quantum cascade lasers integrated on one crystal with a waveguide Talbot filter. In the case of six lasers, the out-of-phase mode or a mixture of the in-phase and out-of-phase modes of the array was generated.

A further development of the concept of filter based on the fractional Talbot effect is the 1–$N$ scheme, in which the length of an external planar waveguide with reflective lateral walls is $L_T/(2N)$. In this waveguide, the beam arriving from a single-mode waveguide is split into $N$ copies (Fig. 6d) [135]. We have found no examples of experimental implementation of such a scheme, but passive 1–$N$ couplers are used in telecom systems.

In a fibre laser with active cores arranged along a ring, a Talbot filter had the form of fibre butt-coupled to the laser, with an RW of certain length and size [136]. Under such conditions, most of the output power was accounted for by the out-of-phase supermode, even though the scatter in the optical length of the cores far exceeded the wavelength. Without an RW, radial diffraction degrades the Talbot effect. Nevertheless, the periodic structure self-reproduction effect makes it possible to ensure the phase locking of the fields in the cores by placing an external plane mirror at a preset distance [137]. Numerical simulation [138] suggests that the use of a concave mirror instead of a plane mirror improves field phase-locking efficiency and reduces diffraction losses.

Lasing in multicore fibres with a hexagonal structure of their active regions and optical coupling between the cores due to field diffraction in a butt-coupled passive multimode fibre was studied by a group at the University of Arizona [139, 140]. Because of the finite size of the outer fibre cladding, the Talbot effect is modified and numerical calculations are needed to find passive fibre parameters at which the highest $Q$ is offered by the in-phase mode. As a result, Li et al. were able to phase-lock the output of fibres having 19 [139] and 37 cores [140], each 7.6 μm in diameter. The beam divergence at $\lambda = 1.5$ μm was 50 and 30 mrad, respectively.

Wrage et al. [141] and Vysotsky et al. [142] described the phase locking of a 5-W 18-core fibre laser having a ring structure. Diffractive coupling between the cores was negligible. Four images of the in-phase mode field emerged distance $L_T/8$ from the fibre end face, one of which was backreflected by a sector mirror in which the number of reflective sectors was the same as the number of cores (Fig. 7a). At an angular width of the mirror sectors equal to a quarter of the period, only one of the four beams was returned. The phase difference between the central and two side beams transmitted through the mirror (Fig. 7b) was $L_T/8$ per period, so that their fields were effectively added in the far field. The angular halfwidth of the output beam in the far field was 12 mrad. Although exceeding the calculated halfwidth of the in-phase mode, this is substantially smaller than that in the case of one core.

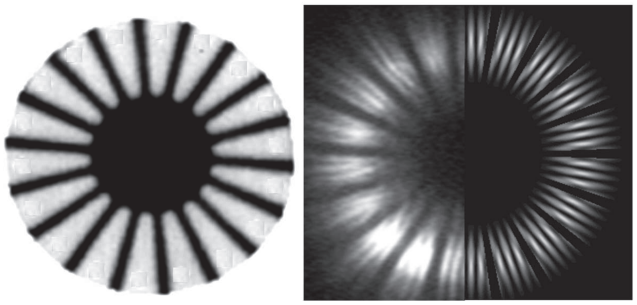

a b

**Figure 7.** (a) Front view of the sector mirror and (b) comparison of experimental data (left side) and calculation results (right side) on the intensity distribution of an 18-core fibre laser behind a mirror located distance $L_T/8$ from the fibre end face [142].

## 5. Theoretical methods for analysis of optically coupled systems

### 5.1. Distributed coupling systems

#### 5.1.1. *T*-matrix method

Characteristics of multielement linear arrays of semiconductor lasers are usually calculated using Maxwell's equations or the wave equation [82, 143]. Along with numerical calculations using Maxwell's equations, an analytical approach based on simplified models of structures was developed. The effective RI (ERI) approximation (see e.g. Ref. [143]) relies on the large difference between the length scales of structures in transverse and lateral directions and reduces to averaging the product of the RI and optical mode profile over the transverse coordinate in the plane of the laser diode at a constant lateral coordinate. As a result of averaging and the use of approximate expressions relating the gain coefficient (GC) to the population inversion in a quantum well (QW), calculation of laser structures reduces to solving a system of 1D equations for the field and inversion density.

In the ERI approximation, the problem of finding a supermode of an antiguided diode laser bar consists in finding eigenfunctions in a planar waveguide with periodic step profiles of the ERI ($n_{\text{eff}}$) and $\Gamma$-factor, which characterises the overlap between the transverse mode and gain profiles. $\Gamma$-factor modulation can be accounted for by field pulling from the active layer to passive waveguides responsible for ERI modulation. The lateral amplitude profile of a $U(x)\exp(\mathrm{i}\beta z)$ field is determined by the equation [41]

$$\frac{\mathrm{d}^2U}{\mathrm{d}x^2}+\left(\frac{\omega^2 n_{\text{eff}}^2}{c^2}-\beta^2\right)U=0, \tag{1}$$

where $\beta$ is the propagation constant; $\omega$ is the emission frequency; and $c$ is the speed of light in vacuum.

Within each period of the structure, the field can be represented as the sum of two linearly independent solutions to Eqn (1): $U = a_l\mathcal{F}(x_l) + b_l\mathcal{G}(x_l)$, where the $x_l$ coordinate is determined within the $l$th cell. The field distributions in the extreme cells of the structure are taken as basis solutions. At the boundaries of the laser bar, the amplitude of the field reflected from the boundary should be zero. The coupling of fields in neighbouring cells is determined by the joining of fields at each index step, which leads to linear recurrent relations for the coefficients of expansion of the field in terms of the basis functions $\mathcal{F}(x_l)$ and $\mathcal{G}(x_l)$:

$$\begin{pmatrix} a_{l+1} \\ b_{l+1} \end{pmatrix} = T\begin{pmatrix} a_l \\ b_l \end{pmatrix}, \tag{2}$$

where the components of the unimodular transfer matrix $T$ can be expressed through the basis functions and their derivatives on cell boundaries [144].

Since any matrix satisfies its secular equation, we can derive an equation relating the amplitudes of the $\mathcal{F}$-wave in three neighbouring cells:

$$a_{l+1} - (\mathrm{Sp}T)a_l + a_{l-1} = 0, \tag{3}$$

where $\mathrm{Sp}T = T_{11} + T_{22}$ is the trace of the matrix. A similar equation is valid for the amplitudes of the $\mathcal{G}$-wave. The general solution to Eqn (3) has the form $a_l = c_1\exp(\mathrm{i}lQ\Lambda) + c_2\exp(-\mathrm{i}lQ\Lambda)$, where $Q$ is the Bloch vector, playing the role of an eigenvalue, and the constants $c_1$ and $c_2$ can be determined from boundary conditions. At $\mathrm{Sp}T = 2$, the equation for $\exp(\mathrm{i}Q\Lambda)$, following from (3), has the doubly degenerate solution $\exp(\mathrm{i}Q\Lambda) = 1$, whereas at $\mathrm{Sp}T = -2$ we have $\exp(\mathrm{i}Q\Lambda) = -1$. These two limits correspond to the in-phase and out-of-phase modes. Side waves resonantly travel through such a periodic structure with a phase shift of $2s\pi$ or $(2s + 1)\pi$ per cell (where $s$ is an integer). In terms of Bloch waves in a periodic crystal, solution degeneracy corresponds to the disappearance of the gap in the spectrum of the waves. Near both resonances, it is convenient to represent Eqn (3) in the form

$$a_{l+1} \pm 2a_l + a_{l-1} = (\mathrm{Sp}T \pm 2)a_l. \tag{4}$$

Even though, formally, diffractive exchange occurs between nearest neighbours, it plays a decisive role at $|\mathrm{Sp}T \pm 2| \ll 1$, because the right-hand side of (4) is small, and leads to effective phase locking of the elements, which is referred to as parallel coupling [41].

The described procedure was brought to analytical expressions [144, 145] for eigenvalues of the in-phase and neighbouring modes of an antiguided linear array as functions of the detuning of parameters of the structure from resonance. In the case of a resonance configuration, the fundamental mode and the neighbouring one turned out to have the same lasing threshold. To ensure discrimination of the neighbouring mode, it is necessary to move away from the resonance structure or introduce absorption in waveguide gaps.

A semiconductor amplifier was analysed in the limit of an infinite lateral size of an array of elements near resonance [146]. In such a case, after the field in the structure passes some distance, dependent on the input profile, the change in field per period of the structure becomes small, which allows the discrete equation (4) to be replaced by a differential equation for the lateral smooth field envelope. As shown earlier [146], in the case of a linear medium without absorption the type of this differential equation in $x$ and $z$ variables changes from elliptic to hyperbolic as resonance is approached. Because of this, an optical field in a resonance array propagates along straight lines at an angle to the optic axis, which depends on the geometric parameters of the structure, in agreement with experimental data [147] on light propagation in a 21-element resonant antiguided array.

In the general case, gain saturation and the associated positive change in RI can lead to field filamentation. It was found [146] that, at relatively low intensities of a field being amplified, self-focusing occurred if the following constraint on the difference $\Delta$ between the ERI step on the waveguide boundary and that corresponding to a resonance structure was fulfilled:

$$\Delta > \frac{\alpha - 1/\alpha}{1 + I/I_{\text{sat}}} g_0 - \frac{\alpha_T}{\alpha}, \tag{5}$$

where $\alpha$ is the line broadening factor; $I$ is the local intensity of the overall field; $I_{\text{sat}}$ is the saturation intensity; $g_0$ is the small-signal GC; and $\alpha_T$ is the absorption coefficient of the waveguide gaps. In the absence of loss modulation, self-focusing develops as the index step on the waveguide boundary rises to above the resonance values, in agreement with calculation results [148].

In numerical simulation of an antiguided diode laser bar, Nabiev et al. [149] found soliton-like solutions in a lateral direction. In Ref. [146], the equation for a smooth envelope was reduced to a generalised Ginzburg–Landau equation, which has solutions in the form of spatially localised structures. The formation of a soliton is due to the fact that the field propagation constant spectrum has forbidden bands at $\Delta > 0$. The dependence of the gain and refractive index on field intensity leads to a shift of the boundaries of the band gap, so that, at a certain combination of parameters, the propagation constant can fall in an allowed band at high intensities. Thus, there is a gap- or Bragg-soliton-like solution (see e.g. Ref. [150] and references therein), which was previously presented in explicit form for near-threshold lasing conditions [146].

### 5.1.2. Transfer equations for single-frequency light

In modelling double-cladding fibre lasers, use is typically made of transfer equations for mode powers. In doing so, radial intensity profiles of optical modes are assumed to be fixed and the local GC is thought to be determined by the total intensity profile [151–153]. In calculations of field propagation in multicore fibre lasers, wide use is made of coupled-mode theory (CMT), in which the field of the optical mode of an entire system (supermode) is represented as a linear combination of optical modes of individual waveguides [154]. The supermode describes the propagation of a beam through a system of passive waveguides in which its shape remains unchanged and only the common phase varies, in proportion to the distance and propagation constant $\beta$.

A multicore fibre usually supports a relatively small number of modes, whose analogues in quantum mechanics are wave functions of coupled states. The supported modes are orthogonal to each other and to leaky modes. In experiments with 7- and 19-core fibres [59, 155], different supermodes of a passive fibre were selectively excited via signal injection from single-mode fibre. Even in the limit of weak interaction between passive cores, CMT poorly describes interaction between higher order supermodes and needs to be modified [156]. The transverse gain nonuniformity, due to either the structure of the gain or its saturation, leads to interaction between supermodes. This interaction is important at field intensities typical of fibre lasers, which are far lower than those characteristic of nonlinear optics. As distinct from CMT, a method based on expansion of the field in terms of exact eigenfunctions (supermodes) allows one to rigorously derive equations for describing the effect of GC distribution nonuniformity on mode competition. Note that, even though distorting mode profiles, thermal effects in fibre have little effect on the interaction between modes and intermodal discrimination [157].

In experiments with a seven-core fibre laser [93], increasing the pump power led to a far-field intensity distribution characteristic of phased fundamental supermode lasing. In-phase mode lasing at high pump power was also observed in the case of pulse amplification in a photonic crystal fibre having seven active cores [97]. In the framework of CMT, Bochove et al. [158] proposed an explanation for spontaneous in-phase mode selection in terms of the dependence of the positive resonant nonlinear part of the RI of glass on pump and lasing intensities. Later, it was found [159] that, in the CMT approximation, phase locking of the field occurred as well in the case of a negative additional nonlinear term in the RI. The nonlinear component of the RI of the fibre core is determined by the difference in polarisability between Yb ions in their ground and excited states and is an intricate function of pump and output intensities [160].

Numerical calculations using the program described by Elkin et al. [161] showed [162] that the phase locking of light in experimental work by Huo et al. [93] was associated with gain nonuniformity due to not only gain saturation but also the structure of the active cores. In those calculations, the simplest model for local GC saturation was used: $g = g_0/(1 + I/I_{\text{sat}})$. The field phase tuning effect was found to become stronger with increasing diffractive coupling between the cores and to be essentially insensitive to index nonlinearity, with allowance for the expected value of the RI. In the case of the design considered by Huo et al. [93], the highest gain corresponded to the out-of-phase mode [163]. At the same time, the result of amplification was highly dependent on conditions at the amplifier input. In particular, if seven beams covering the active cores, with a scatter in phase under 0.3 rad, were directed to the input, the in-phase mode prevailed at the output. This result contradicts the generally accepted view that the mode having the largest small-signal GC prevails at the amplifier output.

The paradox was explained in Refs [164, 165]. In the simplest case, we can consider the competition between two supermodes identical in frequency and polarisation, but having different propagation constants ($\beta_1$ and $\beta_2$) and transverse field distributions [$\psi_1(x,y)$ and $\psi_2(x,y)$]. The total field can then be represented as $E = c_1(z)\psi_1(x,y) + c_2(z)\psi_2(x,y)$, where $c_1(z)$ and $c_2(z)$ are coefficients of expansion of the field in terms of the functions $\psi_1(x,y)$ and $\psi_2(x,y)$, normalised by the condition $\int_S |\psi_i|^2 \mathrm{d}x\mathrm{d}y = 1$ ($i = 1,2$), and the integration is performed over the cross section $S$ of the amplifier. Taking the coefficients in the form $c_{1,2}(z) = \sqrt{P_{1,2}(z)}\exp[\mathrm{i}\phi_{1,2}(z)]$, where $P_{1,2}$ are the powers of the first and second modes, we can obtain the following equations for mode powers and the phase difference of mode fields, $\phi = \phi_2 - \phi_1$:

$$\begin{aligned}
\frac{\mathrm{d}P_1}{\mathrm{d}z} &= G_{11}P_1 + \sqrt{P_1 P_2}\,G_{12}\cos\phi,\\
\frac{\mathrm{d}P_2}{\mathrm{d}z} &= G_{22}P_2 + \sqrt{P_1 P_2}\,G_{12}\cos\phi,\\
\frac{\mathrm{d}\phi}{\mathrm{d}z} &= \beta_2 - \beta_1 - \frac{P_1 + P_2}{\sqrt{P_1 P_2}}G_{12}\sin\phi.
\end{aligned} \tag{6}$$

Here, the $G_{ij}$ matrix elements are the overlap integrals of the mode fields and the GC distribution $g(x,y,z)$:

$$G_{ij}(z) = \int_S \frac{g_0(x,y)\psi_i\psi_j \mathrm{d}x\mathrm{d}y}{1 + P_1\psi_1^2 + P_2\psi_2^2 + 2\psi_1\psi_2\sqrt{P_1P_2}\cos(\phi_i - \phi_j)}, \quad (7)$$

$$i,j = 1,2.$$

The mechanism of competition between longitudinal or transverse modes in a medium with a uniform small-signal GC has been known since studies by Kuznetsova and Rautian [166] and Anan'ev [167], respectively. In such cases, interference between counterpropagating waves leads to gain spatial hole burning and is the key cause of multimode lasing.

Spatial nonuniformity of the GC is represented by additional terms in the system of equations (6), which explicitly relate supermode fields. GC nonuniformity can result from small-signal GC nonuniformity (due to nonuniformity of pumping or doping with active additives) or saturation field nonuniformity. If a small signal coinciding with an optical mode is fed to the input of an amplifier, its propagation will be accompanied by the excitation of another mode as well. The mode cross-coupling effect occurs even in the linear amplification regime, which qualitatively distinguishes it from mode coupling in passive waveguide structures with a nonlinear field dependence of their RI [168].

If the polarisations of two modes having the same frequency are orthogonal to each other, the modes are incoherent with each other, or there is no spatial dependence of the GC, the $G_{12}$ terms in the system of equations (6) are zero. In all these cases, traditional views of mode competition associated with gain saturation remain unchanged. At the same time, even in the case of a standard multimode double-cladding fibre amplifier, the cross-amplification term $G_{12}$ is nonzero, because the small-signal GC is an explicit function of coordinates.

Analysis of the role of cross-amplification in a symmetric waveguide structure [165] shows that the $\sqrt{P_1P_2}G_{12}\cos\phi$ terms in the first two equations in (6) are negative when averaged over $z$. Thus, a given negative contribution from cross-amplification will tell primarily on the lower power mode. As a result, its power may stop growing at all, whereas the higher power mode will continue to build up. Such behaviour of mode powers is illustrated by Fig. 8b, which shows the evolution of the powers of symmetric and antisymmetric modes along the length of an amplifier in a system of two parallel identical thin planar waveguides [164]. In contrast to calculations in the framework of standard transfer equations (cf. to Fig. 8a), Eqns (6) predict a higher gain for the mode whose power is higher at the amplifier input.

In the seven-core fibre laser design described by Huo et al. [93], angular modes essentially do not eliminate the population inversion in the central core. In the case of gain saturation, this causes the in-phase mode, which has the smallest small-signal modal GC, to prevail. Calculations [163] show that, for the in-phase mode to prevail, it is sufficient that, in the field configuration formed in the early stage, the scatter in phase be less than 0.3 rad. The probability of such an event is not low. If it occurs, higher order angular modes with a lower initial power are less amplified, which leads to a better output beam quality [169]. The small-signal modal GC of the in-phase mode exceeds that of the other supermodes [163, 170] if the index step in the central core is reduced, which also can help to select the fundamental mode.

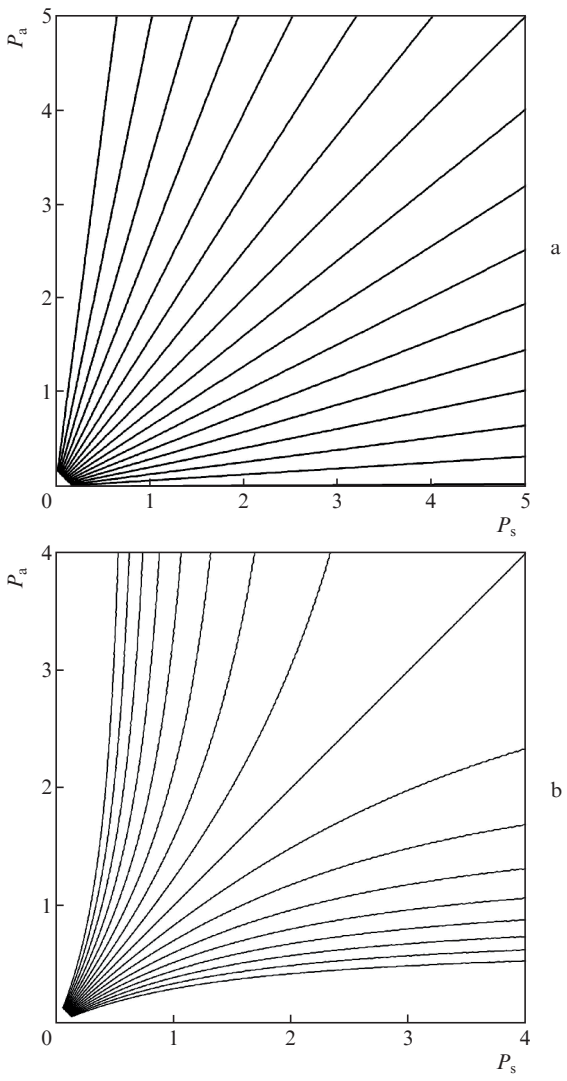


**Figure 8.** Powers of symmetric ($P_s$) and antisymmetric ($P_a$) modes normalised to the saturation power at equal small-signal modal GCs and different relationships between initial powers: (a) incoherent and (b) coherent mode fields [164].

In experiments with a 2-m-long fibre amplifier having a 25-μm core diameter, Andermahr and Fallnich [171] studied the propagation of monochromatic light in the form of a coherent mixture of two spatial modes with different, but not orthogonal, polarisations. At a pump power of ~12.3 W, the fundamental mode prevailed in one plane of polarisation at the amplifier output and the first order mode prevailed in the orthogonal plane. The ideas developed previously [164, 165] allow these results to be understood. Since there is no cross-amplification in the case of fields differing in polarisation, their evolution follows a usual path, with a proportional energy gain for each polarisation. For each polarisation, however, the contribution of the mode with the lower initial power decreases, so that the modes have orthogonal polarisations at the amplifier output [172].

Mode competition was analysed above for a monochromatic field. Four-wave mixing (FWM) can produce fields at frequencies differing from the carrier frequency of the field.

FWM efficiency is limited by the necessity that two conditions be fulfilled for both the frequency difference and propagation constant (frequency and phase matching). Because of this, interaction between waves typically has the form of energy transfer between them. As predicted by Fève [173], the presence of gain in single-mode fibre causes irreversible energy transfer from the stronger wave to the weaker one, even if the phase matching condition is not fulfilled. This effect limits the power of the starting wave, which is accompanied by broadening of the output emission spectrum, as was observed in an experimental study [174]. The coupling between two distinct optical modes in a waveguide through FWM can be described in terms of spatial gain/refraction gratings [175]. Scattering by such gratings leads to power redistribution to higher order modes, degrading the output beam quality [176].

### 5.2. Methods of describing externally coupled systems

The field at the output aperture of an array in externally coupled systems can be represented as

$$u_{\text{out}}(\boldsymbol{r}) = \sum_{m=0}^{N-1} A(m)\exp(\mathrm{i}\varphi_m) f(\boldsymbol{r} - \boldsymbol{r}_m), \tag{8}$$

where $A(m)$ and $\varphi_m$ are the amplitude and phase of the field emitted by the $m$th laser and the function $f(\boldsymbol{r})$ describes the spatial mode field distribution of a single-mode laser centred at a point with transverse coordinate $\boldsymbol{r}_m$. In the case of a steady-state operation of an array of nonidentical lasers, these have the same emission wavelength, but the field amplitudes and phases can vary. The modes of the common cavity of the array can be determined from the condition of field reproduction after a round trip through the cavity (with allowance for amplification). The condition of the reproduction of the system of fields can be reduced to solving a system of equations characterised by a coupling matrix [9]. For a complex field envelope $C(R)$ [i.e. $C(r_m) = A(m)\exp(\mathrm{i}\varphi_m)$ at $R = r_m$] and a beam profile $f(r - r_m)$, which is zero beyond the $m$th single-mode waveguide, the equation representing the condition of field reproduction after a round trip through the entire system has the form

$$\gamma C(\boldsymbol{R}) = B\sum_{R'} M(\boldsymbol{R},\boldsymbol{R}')\, C(\boldsymbol{R}'). \tag{9}$$

Here, the constant $B$ takes into account the total cavity round trip phase change and the gain in the active waveguides; $\gamma$ is the eigenvalue; and $M(\boldsymbol{R},\boldsymbol{R}')$ is the coupling matrix. For an infinite array of identical elements, we have $|\gamma| = 1$.

Theory of Talbot coupling between waveguide lasers in an external cavity of length $L$ in the quasi-optical approximation was developed by Golubentsev et al. [113]. In this theory, the coupling matrix is given by

$$M(\boldsymbol{R},\boldsymbol{R}') = \frac{\mathrm{i}}{\lambda L}\int \mathrm{d}\boldsymbol{\rho}\mathrm{d}\boldsymbol{\rho}' f(\boldsymbol{\rho} - \boldsymbol{R}) f(\boldsymbol{\rho}' - \boldsymbol{R}') \times \exp\left[\frac{\mathrm{i}\pi}{\lambda L}(\boldsymbol{\rho} - \boldsymbol{\rho}')^2\right]. \tag{10}$$

As shown in the limit of a large number of lasers [113], the diffraction loss of the self-reproducing mode in a 1D structure of $N$ lasers with a period $\Lambda$ is $1 - |\gamma|^2 \approx \pi[\Lambda/(Na)]^2$, where $a$ is the radius of the emitting aperture of one laser. The loss in an array of lasers whose output end faces fill a circular aperture has the form $1 - |\gamma|^2 \approx \pi^{-1}[\mu_0\Lambda/(Na)]^2$, where $\mu_0 \approx 2.404$ is the first zero of the zeroth-order Bessel function. The zeroth-order diffraction loss in the array is the same for all modes exactly reproducible in an infinite system (Fig. 4). Even though the in-phase mode in systems of finite size has the lowest loss [177], the difference in loss between the in-phase and other self-reproducing modes is very small, so additional measures should be taken to suppress all modes except the in-phase one.

Golubentsev et al. [113] presented explicit estimates of the loss due to a small tilt ($\theta$) of a plane mirror, $\delta\gamma \approx (\theta a N^2/\lambda)^2$, and a shift ($\delta L$) of the mirror from the position exactly corresponding to the Talbot distance, $|\delta\gamma| \approx \{(\Lambda/a)^2[\delta L/(2\pi L_{\text{T}})]\}^2$. The $a/\Lambda$ ratio characterises the density of filling of a linear aperture with emitters. For a 2D laser array, this density is proportional to $(a/\Lambda)^2$.

In the limit of global coupling in a laser array, where each laser is coupled to the others in the same way [38], all the coupling matrix elements are identical, so that the rank of the matrix is unity. In the case of a positive real-valued coupling coefficient, the in-phase mode is selected. As shown in a review by Likhanskii and Napartovich [9], if the scatter in eigenfrequencies of individual cavities is small compared to the average mode spacing, it has a weak effect on the threshold GC of the other supermodes. One way of ensuring global coupling (see Section 2.6) is through a system of $2 \times 2$ couplers. In the limit of a wavelength common to the entire array, it ensures complete phase locking.

In a scheme with an external Talbot filter, the diffraction loss has a significant effect on the possibility of scaling the system. Wrage et al. [136] proposed a Talbot filter in the form of an RW for a multicore fibre laser with cores arranged along a ring. In the case of a proper adjustment of parameters, the structure of the cores, periodic in the direction of traversal of the RW, ensures zero diffraction loss, as distinct from 1D arrays, which have a finite number of cores. Global coupling between elements is assumed to be possible if the diffractive exchange radius for beam propagation is of the order of the length of the ring. For an RW of length $L_{\text{T}}/4$, this gives the inequality

$$2a/\Lambda < 1/N. \tag{11}$$

In the general case, the field at the output of an $N$-core laser can be represented in the form (8), and the field returned to the system of cores after two passes through the RW can be represented in the form

$$u_{\text{in}}(\boldsymbol{r}) = \sum_{m=0}^{N-1} C_m f(\boldsymbol{r} - \boldsymbol{r}_m).$$

If condition (11) is fulfilled, the following formula for the $C_m$ coefficients can be derived [178];

$$C_m = (-1)^m\left[\frac{1}{N\sqrt{\mathrm{i}}}\sum_{j=0}^{N-1}(-1)^j A(j)\exp(\mathrm{i}\varphi_j)\right]. \tag{12}$$

The distribution of the field returned to the multicore structure (MCS) after two passes through the RW turns out to be out of phase with the amplitudes, equal in magnitude, in all the cores. The field injected into the $j$th core contains a contri-

bution from the output fields in all the cores with identical amplitudes, i.e. the coupling between the cores has a global character. If there is no gain, the eigenvalue of the out-of-phase supermode in the case of nonidentical cores is

$$\gamma = \sum_{j=0}^{N-1} \frac{\exp(\mathrm{i}\varphi_j)}{N\sqrt{\mathrm{i}}}, \tag{13}$$

where $\varphi_j$ is the additional phase after two passes through the $j$th core.

Note that, in their experiments, Wrage et al. [136] observed partial broadening of the regular structure in the output beam distribution. As shown earlier [179], the $2a/\Lambda$ ratio is three times that required by condition (11), so that, if there is a large scatter in the optical length of the cores, two more modes of the MCS have losses comparable to those of the out-of-phase mode.

Another example of optical coupling approaching global coupling in properties is coupling through a cylindrical mirror located the focal length from emitting apertures (the Fourier coupling considered in Section 2.4). In experiments described by Corcoran and Rediker [63] and Corcoran and Durville [64], phase locking with the use of Fourier coupling showed high efficiency and stability to scatter in parameters of individual lasers. The principle of this method [180] is that Fourier transformation converts the field envelope profile of a periodic emitter array into the profile of the field injected into one laser and the field profile of an individual emitter into the total field envelope profile. Global coupling takes place if the quasi-optical approximation is applicable, which limits the size of laser arrays [181].

If the field emitted by a 1D array of $2N + 1$ lasers is represented in the form (8), after light with a resonance wavelength $\lambda_0 = \Lambda^2/F$ travels to a mirror with a focal length $F$ and back the distribution can be represented in the form [182]

$$u_{\mathrm{in}}(x) = \sqrt{\frac{-\mathrm{i}}{\lambda F}}\left[\int_{-\infty}^{\infty} f(x')\exp\left(\frac{-\mathrm{i}kxx'}{2F}\right)\mathrm{d}x'\right]$$

$$\times \sum_{m=-N}^{N} A(m)\exp\left(\mathrm{i}\varphi_m + \frac{2\mathrm{i}\pi xm}{\Lambda}\right), \tag{14}$$

where $k = 2\pi/\lambda_0$ is the wavenumber.

If the field at the output of one element is thought to be a Gaussian beam with a profile $f(x) = \exp(-x^2/a^2)$ and the field envelope is taken in the form of a Gaussian distribution $A(m) = \exp(-m^2\Lambda^2/D^2)$ of width $D$, then, provided the width of the envelope of the field being returned, determined by the Fourier transform of a mode of one element, is matched to the size of the frequency, $\Lambda^2 = \pi Da$, we can obtain [182] an expression for the eigenvalue of the round trip operator:

$$\gamma = \sqrt{\frac{2}{\mathrm{i}\pi}}\frac{\Lambda}{D}\sum_{m=-N}^{N}\exp\left(\mathrm{i}\varphi_m - \frac{2m^2\Lambda^2}{D^2}\right). \tag{15}$$

Thus, even though coupling through a Fourier filter at a large size (and small fill factor) of an array can be thought of as global, the extreme elements of the array make a small contribution to its output power and have a weak effect on phase locking efficiency. Moreover, even if all elements are identical, the diffraction loss in the Fourier filter is nonzero.

## 6. Possible scenarios of total field coherentisation

### 6.1. Steady-state phase locking

The feasibility of steady-state phase locking in a laser array depends on many parameters. The key obstacle to the phase locking of a laser array is the distinction between the eigenfrequencies of individual cavities or, in a more general case, the distinction between the optical lengths of gain elements. In the limit of global coupling between all elements, the phase locking mechanism is based on laser wavelength tuning to a value at which the difference between the gain and loss, both being strong functions of wavelength, is maximal for a considerable fraction of elements [51, 179, 182]. Figure 9 shows a typical dependence of the calculated total field power $P = \int|u_{\mathrm{out}}(x)|^2\mathrm{d}x$ on wavelength detuning $\delta\lambda$ for a laser array. Note that there are peaks roughly equal in power at markedly different wavelengths.

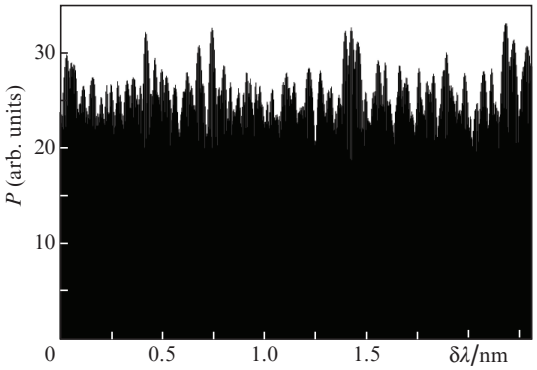


**Figure 9.** Total field power $P$ in an array of 20 ytterbium-doped fibre lasers at a standard deviation of fibre lengths $\sigma(l_m) = 1$ mm (where $l_m$ is the length of the $m$th fibre); gain bandwidth $\delta\lambda_{\max} = 2$ nm; injection power $P_{\mathrm{inj}} = 0.18P_{\mathrm{sat}}$ (where $P_{\mathrm{sat}}$ is the saturation power) [29].

As mentioned in Section 5.2, in the case of a multicore fibre laser with its cores arranged along a ring, global coupling with no diffraction losses can be ensured with the use of a filter in the form of an RW. The eigenvalue for such a structure is described by (13), where the phase shifts $\varphi_j$ are random quantities dependent on the length of the elements and the emission wavelength detuning $\delta\lambda$ from a reference value. At a constant detuning $\delta\lambda$ and parameters typical of fibre lasers, the scatter in $\varphi_j$ far exceeds $2\pi$. The main cause of the scatter in optical lengths in experiments with multicore fibre lasers [136, 137, 141] was the scatter in core radius, which can be quantified by the standard deviation $\Delta r$. At a given MCS, a supermode is generated at the wavelength corresponding to the largest difference between the gain and loss.

Averaging over random MCS's, we can obtain an asymptotic dependence for $\langle|\gamma|^2\rangle$ – the maximum absolute square of the eigenvalue in the gain band $(\lambda_0 - \delta\lambda_{\max}, \lambda_0 + \delta\lambda_{\max})$:

$$\langle|\gamma|^2\rangle \approx \frac{1}{N}\left[C + \ln\left(4NL_{\mathrm{f}}\delta\beta\frac{\delta\lambda_{\max}\Delta r}{\lambda a}\right)\right], \tag{16}$$

where $\delta\beta$ is the average modal correction to the propagation constant and $C \approx 0.577$ is Euler's constant [see derivation of (16) based on extreme value statistics in Ref. [51]].

Direct numerical calculations [178, 179] confirm (Fig. 10) that $\langle|\gamma|^2\rangle$ can be described by the logarithmic relation (16). In the case of identical cores, $\langle|\gamma|^2\rangle$ would be independent of the number of elements. Thus, as the number of cores increases, the phase locking efficiency in a laser array with coupling through a circular Talbot filter decreases as $(\ln N)/N$.

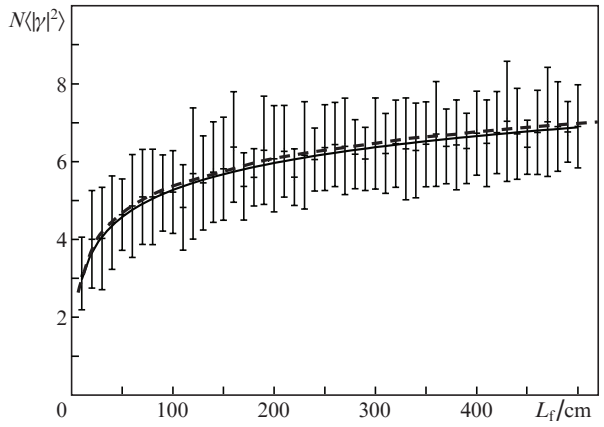


**Figure 10.** Maximum absolute square of the eigenvalue of the out-of-phase mode in the gain band, averaged over 25 MCS's, as a function of MCS length $L_f$. The solid line shows the best fit to the formula $N\langle|\gamma|^2\rangle = \xi + \ln L_f$ ($\xi = 0.67 \pm 0.03$) and the dashed line represents calculation results obtained using (16) [178].

Numerical calculations [182] for a multicore fibre laser with an external Fourier cavity demonstrate that the dependence of the maximum $\langle|\gamma|^2\rangle$ value in the gain band on the scatter in phase shifts in channels is in qualitative agreement with relation (16). For a seven-element array of ytterbium-doped fibre lasers with parameters corresponding to experimental data [64], numerical simulation predicts an almost perfect phase locking, whereas in the case of 15 lasers efficiency is a factor of 2 lower. Thus, even though a Fourier filter offers high selectivity (as pointed out in theoretical analysis by Apollonov et al. [183]), it ensures efficient coupling only in the case of a small laser array with a low fill factor.

### 6.1.1. Phase locking of a system of amplifiers in a common cavity

Fridman et al. [30] analysed 370 000 measurements of the output intensity distribution for an array of 25 ($5 \times 5$) fibre lasers coupled through a system of mirrors in the focal plane [57]. Analysis of an array of output distributions at efficiency maxima in this system indicates that the probability that phase locking efficiency is greater than or equal to $X$ is adequately described by the Bramwell–Holdsworth–Pinton distribution [184]:

$$p(X) = \exp\left\{\kappa\left[\frac{X-\mathcal{A}}{\mathcal{B}} - \exp\left(\frac{X-\mathcal{A}}{\mathcal{B}}\right)\right]\right\}, \qquad (17)$$

where $\mathcal{A}$ and $\mathcal{B}$ are the mean and width of the distribution and the parameter $\kappa$ determines the degree of correlation between the measurements. The best fit was obtained at $\kappa \approx 1.03$. Under the assumption that the distributions at neighbouring spikes are uncorrelated ($\kappa = 1$), distribution (17) reduces to a generalised Fisher–Tippett distribution, which, according to Gnedenko's theorem [185], is an asymptotic probability distribution density for a maximum in a sample of random variables. The probability density for the output power of phase-locked light is well fitted by the Vivo–Majumdar–Bohigas distribution [186] at low efficiencies and by the Majumdar–Vergassola distribution [187] at high efficiencies. These distributions correspond to the distributions of the largest and smallest eigenvalues of random positive matrices.

If a small number of longitudinal modes fall in a gain band, the probability that there is a wavelength common to the array at which a high degree of phase locking can be reached is extremely low. Fibre lasers having a dense spectrum of longitudinal modes are viable candidates for the fabrication of large arrays of phase-locked lasers. It is worth noting that there is practical interest in the ability to simultaneously phase-lock lasers in a few common longitudinal modes, as was observed in experiments [188] concerned with the phase locking of the outputs of four fibre amplifiers in a common cavity with a total round-trip path length of ~820 m. The lasers were coupled using a system of $2 \times 2$ couplers. Two combinations of the differences between the amplifier lengths (measured from the length of the shortest amplifier) were considered: (1) 1.4 cm, 1 m, 5.1 m; (2) 5.1 cm, 1 m, 5.1 m. Measurements of optical and total power oscillation spectra showed that the total spectrum contained structures differing in frequency scale. The largest frequency scale was attributable to the small difference between the amplifier lengths in the two combinations: (1) 17 and (2) 4.8 GHz. In the case of combination 2, the structure was observed to have characteristic spacings between peaks, 200 and 40 MHz, corresponding to length differences of 1 and 5.1 m. Higher resolution measurements showed that each peak was split into a sequence of spikes spaced 240 kHz apart, which corresponded to longitudinal modes of the common cavity. The spikes in turn had a fine structure, which was attributed by Simpson et al. [188] to field polarisation dispersion. Since the generation of a large number of supermodes is accompanied by a considerable broadening of the emission spectrum, the threshold for SBS in the cores decreases markedly, which allows one to envisage a further rise in the power of combined lasers.

To estimate the limiting size of an array in which a high degree of phase locking is highly probable, Kouznetsov et al. [189] proposed a simplified probabilistic approach. Efficiency on the addition of a laser to an existing array was quantified by $\cos\varphi$, where $\varphi$ is the round-trip phase change in the added laser for a field with the supermode wavelength. In the case of an equiprobable distribution, the probability that $\cos\varphi$ exceeds a particular value, $Y$, is $p_1 \approx \sqrt{2(1-Y)}/\pi$. For $N$ lasers with an average length $\bar{L}$, the probability that a given wavelength lies in the gain band $2\pi/\Delta k$ for at least one supermode can be estimated as $\Delta k \bar{L} p_1^{N-1}$, which is valid if this quantity is less than unity. In such a case, the number of lasers that can be phase-locked with a given efficiency is described by the relation

$$N - 1 = 2\ln(\Delta k \bar{L})\left\{\ln\left[\frac{\pi^2}{2(1-Y)}\right]\right\}^{-1}. \qquad (18)$$

It can be obtained from (18) that, at a gain bandwidth of $\sim 10^4$ cm$^{-1}$, up to eight or nine 10-m-long lasers can be phase-locked with a 90% efficiency.

### 6.1.2. Effect of feedback in a gain element on phase locking stability

If there is feedback in each gain element, the laser system is a coupled cavity array. We are interested primarily in stable control over laser operation by an external signal at a small-signal GC above threshold. The laser remains in an external signal-controlled operation mode at any external signal frequency detuning from the frequency of its longitudinal mode if the injection power exceeds the critical one [190]:

$$P_{cr} = \frac{4r_m^2}{(1 - r_m^2)^2}(G_0 - G_{th}), \tag{19}$$

where $G_{th}$ and $G_0$ are the integrated threshold GC and integrated small-signal GC, respectively, and $r_m$ is the reflection coefficient of the output mirror. If the optical power returned to each laser is below the critical one, only some of the lasers in the system will be injection-locked, even at the maximum phase locking efficiency. Under the assumption that all the lasers in an array have identical GCs and injected powers, the injection locking condition can be represented in the form [191]

$$\frac{\eta_{ext}\chi}{1-\chi} \geqslant \frac{4r_m^2}{(1 - r_m^2)^2}\frac{G_0 - G_{th}^{(1)}}{G_0 - G_{th}}, \tag{20}$$

where $G_{th}^{(1)}$ is the integrated threshold GC for an array of identical lasers; $\chi$ is the fraction of the optical power being returned; and $\eta_{ext}$ is the 'true' phase locking efficiency, i.e. the ratio of the output power of the laser array to the input power in the case of identical lasers.

Figure 11 (solid lines) presents numerical simulation results for a fibre laser array with an injection power $P_{inj}$ half the critical one [192]. The number of injection-locked lasers at each random fibre length in the array was determined at the wavelength corresponding to the maximum in $\eta_{ext}$ in the gain band. Next, it was averaged over 200 arrays with a given standard deviation $\sigma(l_m)$. It is seen that, if there is no index nonlinearity, only a small fraction of lasers in a large array are locked by an external signal, even at a phase detuning half the critical one.

The nature of this effect can be understood in terms of a model valid in the limit of a large array [193], in which phase changes in cavities are assumed to be uniformly distributed over the range $(\varphi_c - \delta\varphi, \varphi_c + \delta\varphi)$. It is seen in Fig. 12 that, at a locking efficiency $\eta \approx 80\%$, all the lasers are locked by an external signal. With decreasing phase locking efficiency, the number of states of the array with a given locking efficiency beyond the locking zone increases. This leads to a decrease in the probability that, at a given efficiency, a contribution to the total field will be made by the lasers with a phase change detuning from resonance below the critical one. In other words [194], the density of states of the system in a locked state decreases.

A simplified model for emission phase distributions of individual elements allows one to estimate achievable efficiency for an amplifier array in a common cavity as well [191]. In particular, for the conditions used by Chang et al. [195] in an experiment with 16 fibre amplifiers in a ring configuration, we obtain $\eta = 53\%$, in agreement with the observed value.

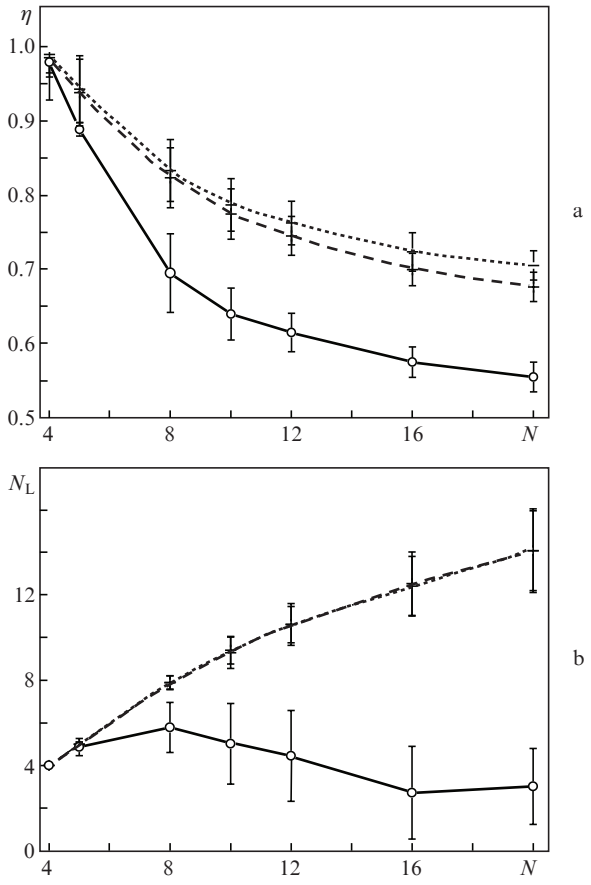


**Figure 11.** Effect of the number of lasers in an array, $N$, on the (a) phase locking efficiency $\eta$ and (b) number of phase-locked lasers $N_L$ averaged over 200 realisations. The solid lines correspond to a line broadening factor $\alpha = 0$ (no index nonlinearity); the long-dashed lines, to $\alpha = 1$; and the short-dashed lines, to $\alpha = -1$. The standard deviation of fibre lengths $\sigma(l_m) = 1$ mm, $G_0 = 3.7$, $P_{inj} = P_{cr}/2$ and $\delta\lambda_{max} = 4$ nm.

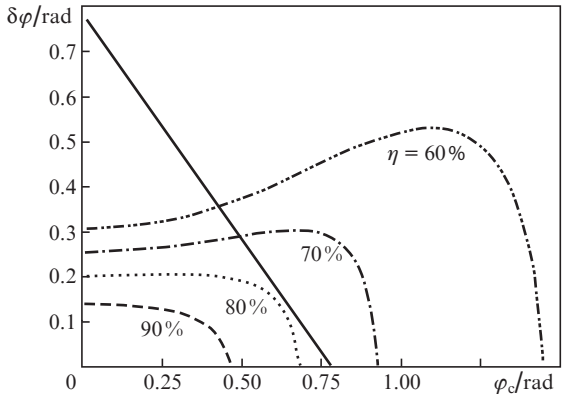


**Figure 12.** Phase locking efficiency ($\eta$) contour lines for a laser array with global coupling at $G_0 = 3.7$ and $P_{inj} = P_{cr}/2$ in the $(\varphi_c, \delta\varphi)$ plane. The phase locking condition for each laser is fulfilled under the straight line [193].

### 6.1.3. Effect of nonlinearity on phase locking stability

The effect of nonlinear variations of the gain and refractive index of media with light intensity on phase locking of gain elements has been the subject of extensive studies. For a model of a laser array with coupling between nearest neigh-

bours, Golubentsev et al. [196] showed that, for stable phase locking in the case of Kerr nonlinear with a coefficient $n_K$, the strength of optical coupling between the lasers, $\mu$, should meet the conditions $\mathrm{Re}\mu > 0$ and $n_K \mathrm{Im}\mu < 0$, i.e. an imaginary term in the coupling strength is needed. Longhi and Feng [197] predicted stable in-phase mode lasing in circular arrays with coupling between nearest neighbours at $\mathrm{Im}\mu = 0$. To this end, the coupling coefficients for clockwise and counterclockwise light propagation in the array should differ and meet a certain relation. We have found no data on experimental implementation of such a type of coupling.

A multichannel ring cavity similar to that schematised in Fig. 2 was considered by Bochove and Shakir [198], who showed that, in this configuration, supermode selection was possible and obtained a logarithmic fit analogous to (16) for the eigenvalue of the supermode. The system was numerically simulated by Bochove et al. [199] at $N = 3$ with allowance for saturable gain in each fibre and the Kerr and resonant nonlinear contributions to the RI. At high pump powers (~1 kW per channel), they found self-oscillation instability of in-phase mode lasing, which was interpreted in terms of a nonlinear contribution to the phase change in an individual cavity [199].

Between 2008 and 2018, Leger presented a series of reports concerned with a double-core fibre having a large separation between its active cores, coupled through an external interferometer. Such a configuration makes it possible to eliminate the effect of the ambient medium on phase locking accuracy. Chiang et al. [200] demonstrated that the RI of a fibre core had a contribution proportional to its GC with a Henry factor $\alpha = 7.4$. This effect can compensate for the phase difference between the fields at the channel outputs, but only if the fields differ significantly in intensity [201]. It was also shown that, in an interference scheme, even slight reflection in the loss channel mitigated the requirements for phase locking accuracy on account of a reduction in intermodal discrimination value [202].

Peleš et al. [203] and Wiesenfeld et al. [204] numerically investigated in-phase mode lasing stability in a system of fibre amplifiers located in a common cavity with global coupling. Population inversion was found using rate equations for three- and four-level media [205], and the mean field in each amplifier was determined using the Rigrod formula. The coupling matrix (9) had a nondegenerate eigenvalue ($M_e$) and an $(N-1)$-fold degenerate eigenvalue ($m_e$). In this model, Peleš et al. [203] derived a system of algebraic equations relating field amplitudes and GCs in fibres after a round trip through a common cavity. As a result, the in-phase supermode turned out to be stable in a few narrow regions in the $(W_p\tau, \zeta)$ plane, where $W_p$ is the pump rate; $\tau$ is the upper level lifetime; and $\cos\zeta = \mathrm{Re}\, M_e m_e^*$ is the coupling parameter. The addition [204] of a shift proportional to the integrated GC to the phase change over fibre improved single-mode lasing stability, but the stability and instability regions persisted.

The effect of index nonlinearity on the phase locking of a laser array locked by an external signal was analysed by Corcoran et al. [206] in the mean field approximation. Generally speaking, there are several solutions for the field in a cavity with a nonlinear medium at a given external signal intensity [207]. Corcoran et al. [206] chose the solution nearest to the eigenmode field. It was shown that the addition to the RI proportional to the gain considerably improved locking efficiency.

Napartovich et al. [192] numerically investigated a laser array with global coupling without resorting to the mean field approximation. The addition of an index component proportional to the gain was shown to slightly improve array phase locking efficiency at any nonlinearity value (Fig. 11a), with a drastic increase in the number of phase-locked lasers. It is seen in Fig. 11b that, even at a large number of lasers in an array, the number of phase-locked lasers continues to rise. As follows from Fig. 13, the likely cause of this effect is the strong dependence of the fraction of phase-locked lasers on efficiency. Figure 13 presents calculation results obtained in a simplified model with a uniform phase scatter distribution in a preset range [29].

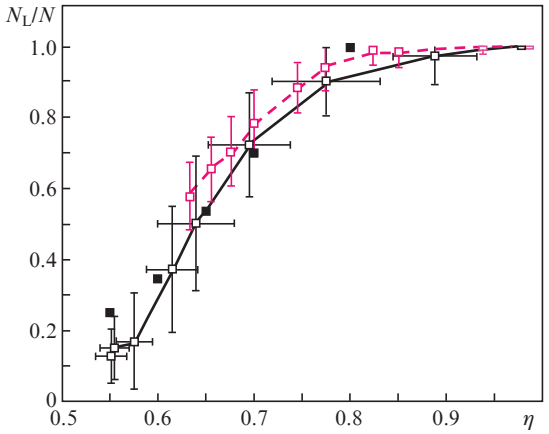


**Figure 13.** Effect of phase locking efficiency on the fraction of supermode-locked lasers averaged over 200 realisations of laser lengths at $\sigma(l_m) = 1$ mm, $G_0 = 3.7$, $P_{inj} = P_{cr}/2$ and $\delta\lambda_{max} = 4$ nm. The solid line corresponds to $\alpha = 0$, and the dashed line, to $\alpha = 1$; the filled squares represent an estimate in a probabilistic approach for $\alpha = 0$ [193].

Modelling in a self-consistent model [191] shows that, at an optimal fraction of the optical power being returned and a nonlinear contribution to the RI, stable phase locking of 20–25 lasers can be expected, with phase locking efficiency $\eta_{ext}$ of ~70%. In Fourier-coupled arrays where the supermode frequency is determined by several lasers located in the centre of the array, Corcoran and Durville [208] were able to achieve in-phase supermode lasing in an array of 35 semiconductor lasers, with an interference pattern contrast of 0.57.

### 6.2. Dynamic operation modes of a laser array

Since the scatter in the optical length of amplifiers has a random character, the degree of phase locking should undergo large fluctuations in response to changes in parameters of the structure that determine optical lengths. Because of this, an undesirable feature of the operation of an optically coupled laser array is a tendency toward spike lasing due to fluctuation-induced random transitions to a different wavelength characterised by a similar difference between the gain and loss [75].

One possible alternative operation mode of practical interest is a transition to regular pulsations of the total output power. The development of periodic pulsations at a varied coupling strength was observed in an experiment with two coupled $CO_2$ lasers [39]. As the frequency of field exchange between their cavities approached the relaxation oscillation frequency, regular oscillations gave way to chaotic ones through an oscillation period doubling sequence. In the cha-

otic pulsation regime, the laser fields retained a high degree of coherence. In the case of two coupled fibre lasers, repetitive pulse generation was observed in a numerical experiment [209] in a wide range of laser coupling coefficients at a constant detuning of the cavity frequencies (200 kHz) and a population inversion relaxation time $\tau_f = 160$ μs. In addition, there was a high far-field interference pattern contrast owing to the coincidence of the field phases of pulses generated at a frequency of $\sim 1/\tau_f$.

The dynamics of the operation of two coupled fibre lasers was addressed in a study reported by Zhou et al. [210], where repetitive pulse generation was due to the phase modulation of one of the lasers at a resonance frequency (23 kHz in the system in question). The resonance frequency is given by

$$\omega_r = \sqrt{\frac{\delta(P_p/P_p^{th} - 1)}{\tau_f \tau_c}}, \quad (21)$$

where $\delta$ is the cavity round trip loss; $\tau_c$ is the cavity round trip time; $P_p$ is the pump power; and $P_p^{th}$ is the threshold pump power. At other modulation frequencies, pulse generation was chaotic.

Dynamic operation modes in laser arrays are typically more complex (see e.g. Ref. [82]). Numerical simulation of the dynamics of the operation of 100- [211] and 1000-element [212] laser arrays with global coupling showed that an increase in the scatter in optical lengths led to spike lasing. At power maxima, the axial brightness was ~30% of the ideal value. This effect emerges if the finite relaxation time of laser level populations is taken into account. For phase locking, it was sufficient that the eigenfrequencies of individual lasers fall in a finite spectral range related to emission frequency uncertainty.

Simultaneous generation of a few longitudinal modes in a ring cavity with two or four fibre amplifiers coupled by $2 \times 2$ couplers was numerically simulated by Wu et al. [213]. The population inversion and mean field in each amplifier were described by rate equations that took into account the Kerr nonlinearity of the RI and group velocity dispersion. The output power rapidly oscillated, and the spectrum contained several narrow lines within a band ~10 GHz in width. The simulation results agree well with experimental data [195]. Note that, for a large number of lasers (10 to 16), the obtained efficiencies exceeded those calculated in a model proposed by Kouznetsov et al. [189].

Sivaramakrishnan et al. [214] numerically investigated the stability of one supermode in a fibre amplifier array located in a common cavity. According to their results, if there is no common longitudinal mode in the gain band of a medium, the power spectrum contains several narrow lines and the order parameter oscillates at a frequency of ~1.8 GHz. If there is only one common mode, as a result of phase perturbation in one of its channels the laser returns to single-mode operation in a few round trips, which is consistent with experimental data reported by Guillot et al. [215]. Kerr nonlinearity leads to line broadening and FWM between modes, increasing the possible number of modes being generated. On the other hand, nonlinearity causes energy leakage to higher loss modes, reducing the power of the fundamental mode.

Nair et al. [216] numerically investigated an array of semiconductor lasers with optical coupling intermediate between global and nearest neighbour coupling. Their results demonstrate that, in the case of identical lasers, taking into account the relaxation of the medium and the time delay in the coupling system leads to synchronous chaotic operation of the entire array, similar to the operation of a single laser in the Lang–Kobayashi model. If the scatter in laser parameters is taken into account [217], the laser array remains phase-locked.

Passive phase locking of pulsed lasers has been studied experimentally by many groups, but for a relatively small number of elements. In an experimental study of three fibre amplifiers in a circular configuration, with light outcoupling through a diffraction grating, Yang et al. [218] observed an interference pattern with a coherence of 0.82 at a pulse repetition rate of 2.2 MHz, peak power of 1.02 kW and pulse duration of 9.6 ns. In a study reported by Rosenstein et al. [219], two photonic crystal fibre amplifiers with a fundamental-mode diameter of 55 μm were interference-coupled with an efficiency $\eta = 92\%$ in a pulse generation mode with a peak power of 0.7 MW. The 10-ns pulse duration and 1-kHz repetition rate were ensured by an acoustic $Q$-switch. In an experimental study of three Nd:YAG lasers coupled by nonlinear gratings in gain elements [71], one laser could operate in the $Q$-switching regime. This also led to an increase in interference pattern contrast.

## 7. Conclusions

Thus, passive phase locking remains a topical approach to obtaining light with high axial brightness. Whereas in the case of systems for specialty applications atmospheric turbulence causes one to choose primarily between active phase locking and incoherent beam combining on a remote target (see e.g. Refs [220, 221] and references therein), in desktop systems active and passive methods compete on equal terms and can be combined [46, 47]. In single-frequency fibre lasers with fixed emission polarisation, the power per amplifier is limited to ~500 W, so that phase locking of even a small number of channels is commercially attractive: both in the case of active phase locking and in a coupling system based on diffractive optical elements, an array output power of ~5 kW has been reached [222]. Issues that remained beyond the framework of this review include methods of laser phase locking in the ultrashort pulse generation regime, in which high peak powers lead to nontrivial physical effects.

Distributed feedback fibre laser systems have evolved into a class of photonic crystal fibres. In semiconductor lasers, distributed feedback has made it possible to couple arrays of hundreds of vertical cavity lasers. At present, there is considerable research effort concentrated on resonant antiguided quantum cascade laser bars emitting in the mid-IR spectral region with several watts of output power [90, 223], but, like in the case of ultrashort pulses, the large emission bandwidth [224] requires novel theoretical approaches.

## References

1. Huang R.K. et al. *IEEE Photonics Technol. Lett.*, **19**, 209 (2007).
2. Sprangle P. et al. *IEEE J. Quantum Electron.*, **45**, 138 (2009).
3. Daneu V. et al. *Opt. Lett.*, **25**, 405 (2000).
4. Fan T.Y. *IEEE J. Sel. Top. Quantum Electron.*, **11**, 567 (2005).
5. Fridman M., Eckhouse V., Davidson N., Friesem A.A. *Opt. Lett.*, **33**, 648 (2008).
6. Andrusyak O. et al. *IEEE J. Sel. Top. Quantum Electron.*, **15**, 344 (2009).
7. Shay T.M. et al. *Proc. SPIE*, **7195**, 71951M (2009).

8. Goodno G.D. et al. *Opt. Lett*., **35**, 1542 (2010).
9. Likhanskii V.V., Napartovich A.P. *Sov. Phys. Usp*., **33**, 228 (1990) [*Usp. Fiz. Nauk*, **160**, 101 (1990)].
10. Glova A.F. *Quantum Electron*., **33**, 283 (2003) [*Kvantovaya Elektron*., **33**, 283 (2003)].
11. Page R.H. et al. *Opt. Lett*., **31**, 353 (2006).
12. Gapontsev D. *Proc. Solid State Diode Laser Technol. Rev*. (Albuquerque, NM, USA, 2008).
13. Krupke W.F. *IEEE J. Sel. Top. Quantum Electron*., **6**, 1287 (2000).
14. Steinhausser B. et al. *Fiber Integr. Opt*., **27**, 407 (2008).
15. Flushe B.M., Alley T.G., et al. *Opt. Express*, **14**, 11748 (2006).
16. Goldobin I.S., Evtikheev N.N., Plyavenek A.G. *Sov. J. Quantum Electron*., **19**, 1261 (1989) [*Kvantovaya Elektron*., **16**, 1957 (1989)].
17. Lim J.J. et al. *IEEE J. Sel. Top. Quantum Electron*., **15**, 993 (2009).
18. Stickley C.M. et al. *Tech. Dig. Adv. Solid-State Photonics Conf*. (Incline Village, Nevada, USA, 2006) TuA1.
19. Apollonov V.V. et al. *Quantum Electron*., **29**, 839 (1999) [*Kvantovaya Elektron*., **29**, 1 (1999)].
20. Wacks M., Ryan L., Johannsen D., Geopfarth R. *J. Directed Energy*, **1**, 317 (2006).
21. Aleksandrov B.P. et al. *Quantum Electron*., **33**, 25 (2003) [*Kvantovaya Elektron*., **33**, 25 (2003)].
22. Giesen A., Speiser J. *IEEE J. Sel. Top. Quantum Electron*., **13**, 598 (2007).
23. Beil K. et al. *Opt. Express*, **18**, 20712 (2010).
24. Mende J. et al. *Proc. SPIE*, **7193**, 71931V (2009).
25. Richardson D.J., Nilsson J., Clarkson W.A. *J. Opt. Soc. Am. B*, **27**, B64 (2010).
26. Dawson J. et al. *Opt. Express*, **16**, 13240 (2008).
27. Smith A.V. et al. *IEEE J. Sel. Top. Quantum Electron*., **15**, 153 (2009).
28. Augst S.J. et al. *J. Opt. Soc. Am. B*, **24**, 1707 (2007).
29. Vysotsky D.V., Elkin N.N., Napartovich A.P. *Quantum Electron*., **40**, 861 (2010) [*Kvantovaya Elektron*., **40**, 861 (2010)].
30. Fridman M. et al. *Phys. Rev. E: Stat., Nonlinear, Soft Matter Phys*., **86**, 041142 (2012).
31. Glova A.F. et al. *Quantum Electron*., **28**, 851 (1998) [*Kvantovaya Elektron*., **25**, 875 (1998)].
32. Vasil'ev A.F. et al. *Sov. J. Tech. Phys*., **31**, 191 (1986) [*Zh. Tekh. Fiz*., **56**, 312 (1986)].
33. Bogachev V.A. et al. *Quantum Electron*., **42** (6), 531 (2012) [*Kvantovaya Elektron*., **42** (6), 531 (2012)].
34. Basov N.G., Belenov E.M., Letokhov V.S. *Zh. Tekh. Fiz*., **35**, 1098 (1965).
35. Perel' V.I., Rogova I.V. *Opt. Spektrosk*., **25**, 716 (1968).
36. Perel' V.I., Rogova I.V. *Opt. Spektrosk*., **25**, 943 (1968).
37. Spencer M.B., Lamb W.E. Jr. *Phys. Rev. A*, **5**, 893 (1972).
38. Fader W.J., Palma G.E. *Opt. Lett*., **10**, 381 (1985).
39. Bondarenko A.V. et al. *J. Exp. Theor. Phys*., **68**, 461 (1989) [*Zh. Eksp. Teor. Fiz*., **95**, 807 (1989)].
40. Roy R. *AIP Conf. Proc*., **548**, 260 (2000).
41. Botez D., in *Diode Laser Arrays* (Cambridge: Cambridge Univ. Press, 1994) pp 1–71.
42. Mafi A., Moloney J.V. *J. Opt. Soc. Am. B*, **21**, 897 (2004).
43. Veldkamp W.B., Leger J.R., Swanson G.J. *Opt. Lett*., **11**, 303 (1986).
44. Leger J.R., Swanson G.J., Veldkamp W.B. *Appl. Phys. Lett*., **48**, 888 (1986).
45. Morel J., Woodtli A., Dändliker R. *Opt. Lett*., **18**, 1520 (1993).
46. Schimmel G. et al. *Proc. SPIE*, **9733**, 97330I (2016).
47. Schimmel G. et al. *Proc. SPIE*, **10086**, 100860O (2017).
48. Redmond S.M. et al. *Opt. Lett*., **37**, 2832 (2012).
49. Thielen P.A. et al. *Opt. Lett*., **37**, 3741 (2012).
50. Derzhavin S.I., Dyukel' O.A., Lyndin N.M. *Quantum Electron*., **42** (6), 561 (2012) [*Kvantovaya Elektron*., **42** (6), 561 (2012)].
51. Gerasimov V.B. et al. *Sov. J. Quantum Electron*., **16**, 839 (1986) [*Kvantovaya Elektron*., **13**, 1278 (1986)].
52. Gerasimov V.B. et al. *Sov. J. Quantum Electron*., **17**, 579 (1987) [*Kvantovaya Elektron*., **14**, 912 (1987)].
53. He B. et al. *Opt. Express*, **14**, 2721 (2006).
54. Wan C., Tiffany B., Leger J.R. *IEEE J. Quantum Electron*., **47**, 770 (2011).
55. Aleksandrov B.P. et al. *Sov. J. Quantum Electron*., **20**, 1370 (1990) [*Kvantovaya Elektron*., **17**, 1462 (1990)].
56. Rediker R.H., Corcoran C.J., Pang L.Y., Liew S.K. *IEEE J. Quantum Electron*., **25**, 1547 (1989).
57. Fridman M., Nixon M., Davidson N., Friesem A. *Opt. Lett*., **35**, 1434 (2010).
58. Lhermite J. et al. *Opt. Lett*., **32**, 1842 (2007).
59. Shalaby B.M. et al. *Appl. Phys. B*, **100**, 859 (2010).
60. Shalaby B.M. et al. *Appl. Phys. B*, **105**, 213 (2011).
61. Yang Y. et al. *Opt. Lett*., **39**, 708 (2014).
62. Liu H. et al. *J. Lightwave Technol*., **32**, 2220 (2014).
63. Corcoran C.J., Rediker R.H. *Appl. Phys. Lett*., **59**, 759 (1991).
64. Corcoran C.J., Durville F. *Appl. Phys. Lett*., **86**, 201118 (2005).
65. Likhanskii V.V., Napartovich A.P., Sukharev A.G. *Sov. J. Quantum Electron*., **17**, 1105 (1987) [*Kvantovaya Elektron*., **14**, 1733 (1987)].
66. Baranov V.Yu. et al. *Sov. J. Quantum Electron*., **18**, 1462 (1988) [*Kvantovaya Elektron*., **15**, 2335 (1988)].
67. Bondarenko A.V. et al. *Sov. J. Quantum Electron*., **18**, 563 (1988) [*Kvantovaya Elektron*., **15**, 877 (1988)].
68. Basiev T.T. et al. *Quantum Electron*., **33** (8), 659 (2003) [*Kvantovaya Elektron*., **33** (8), 659 (2003)].
69. Basiev T.T. et al. *Quantum Electron*., **37**, 143 (2007) [*Kvantovaya Elektron*., **37**, 143 (2007)].
70. Basiev T.T. et al. *Quantum Electron*., **39**, 31 (2009) [*Kvantovaya Elektron*., **39**, 31 (2009)].
71. Basiev T.T. et al. *Quantum Electron*., **41**, 207 (2011) [*Kvantovaya Elektron*., **41**, 207 (2011)].
72. Lyndin N.M. et al. *Quantum Electron*., **24**, 1058 (1994) [*Kvantovaya Elektron*., **21**, 1141 (1994)].
73. Shirakawa A., Saitou T., Sekiguchi T., Ueda K. *Opt. Express*, **10**, 1167 (2002).
74. Sabourdy D. et al. *Opt. Express*, **11**, 87 (2003).
75. Shirakawa A., Matsuo K., Ueda K. *Tech. Dig. CLEO 2004* (San Francisco, USA, 2004) CThGG2.
76. Bruesselbach H. et al. *Tech. Dig. CLEO 2005* (Baltimore, USA, 2005) CMDD4.
77. Wang B., Mies E., Minden M., Sanchez A. *Opt. Lett*., **34** (7), 863 (2009).
78. Kabeya D. et al. *Opt. Express*, **23** (4), 5035 (2015).
79. Ishaaya A.A., Davidson N., Friesem A.A. *IEEE J. Sel. Top. Quantum Electron*., **15**, 301 (2009).
80. Zhao P. et al. *Opt. Express*, **26**, 18019 (2018).
81. Purnawirman, Phua P.B. *Opt. Express*, **19**, 5364 (2011).
82. Winful H.G., Defreez R., in *Diode Laser Arrays* (Cambridge: Cambridge Univ. Press, 1994) pp 226–254.
83. Botez D. *Proc. IEE. Part J. Optoelectronics*, **139**, 14 (1992).
84. Mawst L.J. et al. *Appl. Phys. Lett*., **60**, 668 (1992).
85. Yang H. et al. *Electron. Lett*., **33**, 136 (1997).
86. Yang H., Mawst L.J., Botez D. *Appl. Phys. Lett*., **76**, 1221 (2000).
87. Bao L. et al. *Appl. Phys. Lett*., **84**, 320 (2004).
88. Bao L. et al. *IEEE J. Sel. Top. Quantum Electron*., **11**, 968 (2005).
89. Kirch J.D. et al. *Appl. Phys. Lett*., **106**, 061113 (2015).
90. Sigler C. et al. *IEEE J. Sel. Top. Quantum Electron*., **23**, 1200706 (2017).
91. Glas P. et al. *Opt. Commun*., **151**, 187 (1998).
92. Elkin N.N. et al. *Opt. Commun*., **177**, 207 (2000).
93. Huo Y. et al. *IEEE Photonics Technol. Lett*., **13**, 439 (2001).
94. Huo Y., Cheo P.K., King G.G. *Opt. Express*, **12**, 6230 (2004).
95. Russel P.St.J. *J. Lightwave Technol*., **24**, 4729 (2006).
96. Michaille L. et al. *IEEE J. Sel. Top. Quantum Electron*., **15**, 328 (2009).
97. Fang X.H. et al. *Opt. Lett*., **35**, 2326 (2010).
98. Fang X. et al. *Opt. Lett*., **36**, 1005 (2011).
99. Hu M.L. et al. *J. Mod. Opt*., **58**, 1966 (2011).
100. Beach R.J. et al. *J. Opt. Soc. Am. B*, **19**, 1521 (2002).
101. Beach R.J. et al. *IEEE Photonics Technol. Lett*., **15**, 670 (2003).
102. Vysotsky D.V., Napartovich A.P., Trapeznikov A.G. *Quantum Electron*., **33**, 1089 (2003) [*Kvantovaya Elektron*., **33**, 1089 (2003)].
103. Dawson J.W. et al. US Patent 2004/0247272 A1 (2004).
104. Drachenberg D. et al. *Opt. Express*, **21**, 18089 (2013).
105. Drachenberg D.R. et al. *Opt. Express*, **21**, 11257 (2013).
106. Anderson B. et al. *Opt. Lett*., **39**, 6498 (2014).
107. Napartovich A.P., Elkin N.N., Vysotsky D.V. *Tech. Dig. CLEO 2013* (San Jose, Ca, USA, 2013, OSA) CTu2K.5.
108. Elkin N.N., Napartovich A.P., Vysotsky D.V. *Proc. Int. Conf. on Advanced Optoelectron. and Lasers (CAOL'2013)* (Sudak, Ukraine, IEEE, 2013) pp 38–40.
109. Sha P. et al. *Opt. Lett*., **35**, 2329 (2010).
110. Talbot H.F. *Philos. Mag.*, **9**, 401 (1836).

111. Lord Rayleigh. *Philos. Mag*., **11**, 196 (1881).
112. Antyukhov V.V. et al. *JETP Lett*., **44**, 78 (1986) [*Pis'ma Zh. Eksp. Teor. Fiz*., **44**, 63 (1986)].
113. Golubentsev A.A., Likhanskii V.V., Napartovich A.P. *J. Exp. Theor. Phys*., **66**, 676 (1987) [*Zh. Eksp. Teor. Fiz*., **93**, 1199 (1987)].
114. D'Amato F.X., Siebert E.T., Roychoudhuri V. *Proc. SPIE*, **1043**, 100 (1989).
115. Glova A.F. et al. *Quantum Electron*., **26**, 614 (1996) [*Kvantovaya Elektron*., **23**, 630 (1996)].
116. Apollonov V.V. et al. *Quantum Electron*., **28**, 344 (1998) [*Kvantovaya Elektron*., **25**, 355 (1998)].
117. Mawst L.J. et al. *Electron. Lett*., **25**, 365 (1989).
118. Jia Z. et al. *Appl. Phys. Lett*., **111**, 061108 (2017).
119. Napartovich A.P., Elkin N.N., Vysotsky D.V. *Proc. SPIE*, **4184**, 431 (2001).
120. Winthrop J.T., Worthington C.R. *J. Opt. Soc. Am.*, **55**, 373 (1965).
121. Leger J.R., Griswold M.P. *Appl. Phys. Lett.*, **56**, 4 (1990).
122. Golubentsev A.A. et al. *Sov. J. Quantum Electron*., **20**, 934 (1990) [*Kvantovaya Elektron*., **17**, 1018 (1990)].
123. Vasil'tsov V.V. et al. *Proc. SPIE*, **2109**, 122 (1993).
124. Tradonsky C. et al. *Appl. Opt*., **56**, A126 (2017).
125. Paboeuf D. et al. *J. Opt. Soc. Am. B*, **28** (5), 1289 (2011).
126. Liu B., Braiman Y. *Opt. Commun*., **414**, 202 (2018).
127. Kandidov V.P., Terekhova I.V. *Quantum Electron*., **33**, 536 (2003) [*Kvantovaya Elektron*., **33**, 536 (2003)].
128. Corcoran C.J., Durville F. *Opt. Lett.*, **40** (13), 2957 (2015).
129. Rivlin L.A., Shul'dyaev V.S. *Izv. Vyssh. Uchebn. Zaved., Ser. Radiofiz*., **11**, 572 (1968).
130. Ulrich R., Ankele G. *Appl. Phys. Lett*., **27**, 337 (1975).
131. Grigor'eva E.E., Semenov A.T. *Sov. J. Quantum Electron*., **8**, 1063 (1978) [*Kvantovaya Elektron*., **5**, 1877 (1978)].
132. Soldano L.B., Pennings E.C.M. *J. Lightwave Technol*., **13**, 615 (1995).
133. Wang L. et al. *Opt. Express*, **24**, 30275 (2016).
134. Meng B. et al. *Opt. Express*, **25**, 3077 (2017).
135. Banerji J., Davies A.R., Jenkins R.M. *Appl. Opt*., **36**, 1604 (1997).
136. Wrage M. et al. *Opt. Commun*., **205**, 367 (2002).
137. Wrage M. et al. *Opt. Lett.*, **25**, 1436 (2000).
138. Vysotsky D.V., Napartovich A.P. *Quantum Electron*., **31**, 298 (2001) [*Kvantovaya Elektron*., **31**, 298 (2001)].
139. Li L. et al. *Opt. Lett*., **31** (17), 2577 (2006).
140. Li L. et al. *J. Opt. Soc. Am. B*, **24**, 1721 (2007).
141. Wrage M. et al. *Opt. Lett*., **26**, 980 (2001).
142. Vysotsky D.V. et al. *Proc. SPIE*, **4751**, 395 (2002).
143. Hadley G.R., in *Diode Laser Arrays* (Cambridge: Cambridge Univ. Press, 1994) pp 180–225.
144. Botez D., Napartovich A.P. *IEEE J. Quantum Electron*., **30**, 975 (1994).
145. Botez D., Napartovich A.P., Zmudzinski C.A. *IEEE J. Quantum Electron*., **31**, 244 (1995).
146. Vysotsky D.V., Napartovich A.P. *J. Exp. Theor. Phys*., **88**, 227 (1999) [*Zh. Eksp. Teor. Fiz*., **155**, 416 (1999)].
147. Zmudzinski C.A., Botez D., Mawst L.J., Bhattacharya A., Nesnidal M., Nabiev R.F. *IEEE J. Sel. Top. Quantum Electron*., **1**, 129 (1995).
148. Nabiev R.F., Botez D. *IEEE J. Sel. Top. Quantum Electron*., **1**, 138 (1995).
149. Nabiev R.F., Yeh P., Botez D. *Opt. Lett*., **18**, 1612 (1993).
150. Kivshar Yu.S., Agrawal G.P. *Optical Solitons: From Fibers to Photonic Crystals* (London: Academic 2003; Moscow: Fizmatlit, 2005) Ch. 5.
151. Huo Y., Cheo P.K. *J. Opt. Soc. Am. B*, **22**, 2345 (2005).
152. Gong M., Lu C., Yan P., Wang Y. *IEEE J. Quantum Electron*., **44**, 1009 (2008).
153. Jiang Z., Marciante J.R. *J. Opt. Soc. Am. B*, **25**, 247 (2008).
154. Yariv A. *IEEE J. Quantum Electron.*, **9**, 919 (1973).
155. Shalaby B.M. et al. *Appl. Phys. B*, **97**, 599 (2009).
156. Xia C. et al. *IEEE J. Sel. Top. Quantum Electron*., **22**, 196 (2016).
157. Poli F., Laegsgaard J., et al. *J. Lightwave Technol*., **37**, 1075 (2019).
158. Bochove E.J., Cheo P.K., King G.G. *Opt. Lett*., **28**, 1200 (2003).
159. Bochove E.J. *Proc. SPIE*, **5708**, 132 (2005).
160. Antipov O.L. et al. *Quantum Electron*., **36**, 418 (2006) [*Kvantovaya Elektron*., **36**, 418 (2006)].
161. Elkin N.N. et al. *Opt. Commun*., **177**, 207 (2000).
162. Vysotsky D.V., Elkin N.N., Napartovich A.P. *Quantum Electron*., **36**, 73 (2006) [*Kvantovaya Elektron*., **36**, 73 (2006)].
163. Elkin N.N. et al. *Opt. Commun*., **277**, 390 (2007).
164. Napartovich A.P., Vysotsky D.V. *Phys. Rev. A*, **76**, 063801 (2007).
165. Vysotsky D.V., Napartovich A.P. *J. Exp. Theor. Phys*., **108**, 547 (2009) [*Zh. Eksp. Teor. Fiz*., **135**, 627 (2009)].
166. Kuznetsova T.I., Rautian S.G. *Sov. Phys. Solid State*, **5**, 1535 (1964) [*Fiz. Tverd. Tela*, **5**, 2105 (1963)].
167. Anan'ev Yu.A. *Zh. Tekh. Fiz*., **37**, 139 (1967).
168. Mayer A.A. *Phys. Usp*., **38**, 991 (1995) [*Usp. Fiz. Nauk*, **165**, 1037 (1995)].
169. Elkin N.N. et al. *J. Lightwave Technol*., **25**, 4729 (2007).
170. Gundu K.M., Kolesik M., Moloney J.V. *Opt. Lett*., **32**, 763 (2007).
171. Andermahr N., Fallnich C. *Opt. Express*, **16**, 8678 (2008).
172. Andermahr N., Fallnich C. *Opt. Express*, **16**, 20038 (2008).
173. Fève J.-P. *Opt. Express*, **15**, 577 (2007).
174. Fève J.-P. et al. *Opt. Express*, **15**, 4647 (2007).
175. Antipov I.L. et al. *Quantum Electron*., **36**, 418 (2006) [*Kvantovaya Elektron*., **36**, 418 (2006)].
176. Smith A.V., Smith J.J. *Opt. Express*, **19**, 11318 (2011).
177. Golubentsev A.A., Likhanskii V.V., Napartovich A.P. *Izv. Vyssh. Uchebn. Zaved., Ser. Radiofiz*., **32**, 417 (1989).
178. Vysotsky D.V. et al. *Quantum Electron*., **32**, 271 (2002) [*Kvantovaya Elektron*., **32**, 271 (2002)].
179. Napartovich A.P., Vysotsky D.V. *J. Mod. Opt*., **50**, 2715 (2003).
180. Liu L. *J. Phys. A: Math. Gen*., **27**, L285 (1994).
181. Corcoran C.J., Pasch K.A. *J. Phys. A: Math. Gen*., **37**, L461 (2004).
182. Vysotsky D.V., Napartovich A.P., Troshchieva V.N. *Quantum Electron*., **37**, 345 (2007) [*Kvantovaya Elektron*., **37**, 345 (2007)].
183. Apollonov V.V., Kislov V.I., Prokhorov A.M. *Quantum Electron*., **26**, 1051 (1996) [*Kvantovaya Elektron*., **23**, 1081 (1996)].
184. Bramwell S.T. et al. *Phys. Rev. Lett*., **84**, 3744 (2000).
185. Gumbel E.J. *Statistics of Extremes* (New York: Columbia Univ. Press, 1958; Moscow: Mir, 1985).
186. Vivo P., Majumdar S.N., Bohigas O. *J. Phys. A*, **40**, 4317 (2007).
187. Majumdar S.N., Vergassola M. *Phys. Rev. Lett*., **102**, 060601 (2009).
188. Simpson T.B. et al. *Opt. Express*, **15**, 11731 (2007).
189. Kouznetsov D. et al. *Opt. Rev*., **12**, 445 (2005).
190. Gordon R. *IEEE J. Quantum Electron*., **42**, 353 (2006).
191. Napartovich A.P., Elkin N.N., Vysotsky D.V. *Appl. Opt*., **53**, I23 (2014).
192. Napartovich A.P., Elkin N.N., Vysotsky D.V. *Proc. SPIE*, **7914**, 791428 (2011).
193. Vysotsky D.V., Elkin N.N., Napartovich A.P. *Quantum Electron*., **43**, 845 (2013) [*Kvantovaya Elektron*., **43**, 845 (2013)].
194. Corcoran C.J., Durville F., Ray W. *IEEE J. Quantum Electron*., **47**, 1043 (2011).
195. Chang W.Z. et al. *Tech. Dig. CLEO 2009* (San Francisco, USA, 2009) JTuD63.
196. Golubentsev A.A., Likhanskii V.V., Napartovich A.P. *Sov. J. Quantum Electron*., **19**, 477 (1989) [*Kvantovaya Elektron*., **16**, 730 (1989)].
197. Longhi S., Feng L. *Appl. Phys. Lett. Photonics*, **3**, 060802 (2018).
198. Bochove E.J., Shakir S.A. *IEEE J. Sel. Top. Quantum Electron*., **15**, 320 (2009).
199. Bochove E.J. et al. *IEEE J. Quantum Electron*., **47**, 777 (2011).
200. Chiang H.-S. et al. *Opt. Lett*., **40** (6), 962 (2015).
201. Kunkel W.M., Leger J.R. *Opt. Express*, **26** (7), 9373 (2018).
202. Khajavikhan M., Leger J.R. *IEEE J. Sel. Top. Quantum Electron*., **15** (2), 281 (2009).
203. Peleš S., Rogers J.L., Wiesenfeld K. *Phys. Rev. E*, **73**, 026212 (2006).
204. Wiesenfeld K., Peleš S., Rogers J.L. *IEEE J. Sel. Top. Quantum Electron*., **15**, 312 (2009).
205. Ray W., Wiesenfeld K., Rogers J.L. *Phys. Rev. E*, **78**, 046203 (2008).
206. Corcoran C.J., Durville F., Pasch K.A. *IEEE J. Quantum Electron*., **44**, 275 (2008).
207. Felber F.S., Marburger J.H. *Appl. Phys. Lett*., **26**, 731 (1976).
208. Corcoran C.J., Durville F. *Opt. Express*, **22**, 8420 (2014).

209. Nixon M. et al. *Opt. Lett*., **36**, 1320 (2011).
210. Zhou P. et al. *Chin. Opt. Lett*., **6**, 523 (2008).
211. Kourchatov S.Yu., Likhanskii V.V., Napartovich A.P. *J. Exp. Theor. Phys*., **80**, 833 (1995) [*Zh. Eksp. Teor. Fiz*., **107**, 1491 (1995)].
212. Kourchatov S.Yu. et al. *Phys. Rev. A*, **52**, 4089 (1995).
213. Wu T.W. et al. *Opt. Express*, **17**, 19509 (2009).
214. Sivaramakrishnan S. et al. *IEEE J. Quantum Electron*., **51**, 1600209 (2015).
215. Guillot J. et al. *Opt. Lett*., **36**, 2907 (2011).
216. Nair N., Bochove E., Braiman Y. *Opt. Express*, **26**, 20040 (2018).
217. Nair N., Bochove E., Braiman Y. *Opt. Commun*., **430**, 104 (2019).
218. Yang Y.-F. et al. *Chin. Phys. Lett*., **31**, 084206 (2014).
219. Rosenstein B., Shirakov A., Belker D., Ishaaya A.A. *Opt. Express*, **22** (6), 6416 (2014).
220. Nelson W., Shprangle P., Davis C.C. *Appl. Opt*., **55** (29), 8338 (2016).
221. Sprangle P. et al. *Appl. Opt*., **56** (16), 4825 (2017).
222. Liu Z.J. et al. *Sci. China Inf. Sci*., **62** (4), 041301 (2019).
223. Elkin N.N. et al. *IEEE J. Quantum Electron*., **55** (3), 2300210 (2019).
224. Sigler C. et al. *Opt. Eng.*, **57** (1), 011013 (2018).